JOHANNES KEPLER UNIVERSITÄT LINZ | JKU

TNF

Technisch-Naturwissenschaftliche

Fakultät

Photochemical Reduction of Redox Cofactors using Cobaloxime Complexes as Hydrogenation Catalysts

REPORT TO THE AUSTRIAN MARSHALL PLAN FOUNDATION

Author:

Dr. Kerstin T. Oppelt

kerstin.oppelt@jku.at

Supervisors:

Prof. Dr. Günther Knör (JKU)

Dr. Etsuko Fujita (BNL)

In the visit of

The Artificial Photosynthesis Group

Chemistry Department

Brookhaven National Laboratory

Table of Contents

Abstract

The project investigates the applicability of water soluble (metallo)porphyrins and -chlorins for the photochemical reduction of the redox cofactor NADH in combination with cobalt dimethylglyoxime complexes. The research is focused on two component systems similar to the one depicted in Figure 1 where, in a proposed catalytic cycle, a metallo-chlorin is used as a Photosensitizer (**PS**) and a redox catalyst (Co-Complex) forms the desired product NADH from NAD^+ applying a sacrificial electron donor (D) such as TEOA or others. The NADH formed is further used to reduce carbon dioxide to formate using formate dehydrogenase (FDH).

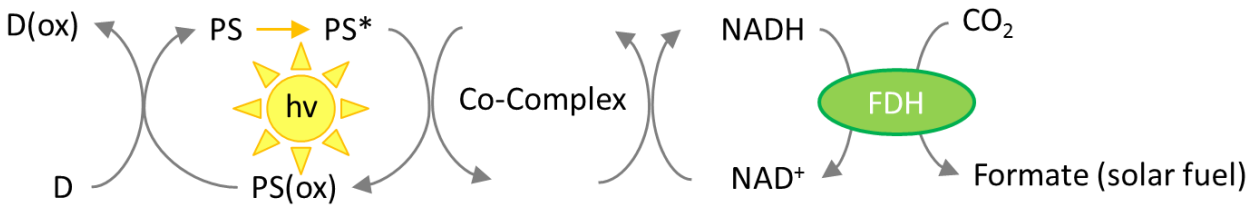

Figure 1 Scheme of the investigated photoreaction: D sacrificial electron donor, PS photosensitizer metalloporphyrins and –chlorins as well as other dyes; Co-Complex: hydrogen evolving/ hydride transfer catalyst cobaloxime, FDH: formate dehydrogenase

Introduction and Scientific Background

Artificial Photosynthesis and solar fuel product has become a wide field of investigation in recent years. The focus of this work lies within mimics of photosystem I (PS I) as it occurs in green plant chloroplasts –in as part of the reductive side of the photosynthetic light reaction.

The light reaction in natural photosynthesis can be separated into two parts as shown in Figure 2. Light-mediated water oxidation occurs at photosystem II (P 680) (green box). The main reaction takes place at the reactive site of photosensitizers a bigger protein structure containing a Mn_4Ca-cluster situated in the oxygen evolving complex, the OEC.[1,2] Water is oxidized and oxygen is formed alongside with two protons and two electrons per each H_2O molecule. The electrons are transferred to photosystem I (P 700) which is shown in the red box of Figure 2. Here the fuel generating reductive partial reactions takes place, using light as an energy source. Protons and electrons originating from the oxidized water molecules are transferred and combined to generate NAD(P)H. This molecule works as an intermediate energy carrier for storage and transportation of reductive equivalents required for subsequent carbon dioxide fixation processes.

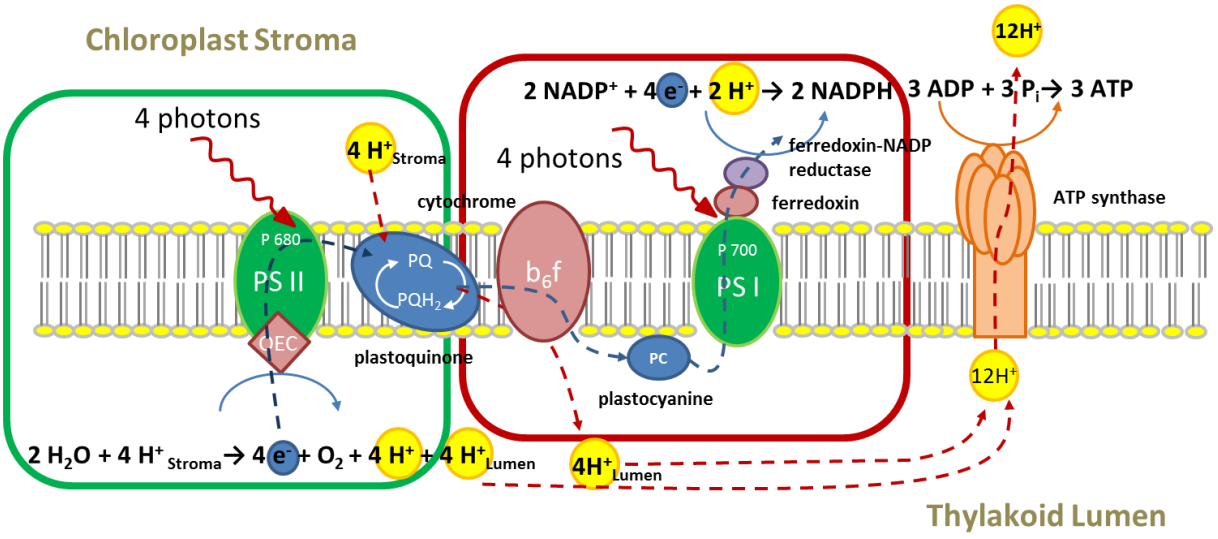

Figure 2 Scheme of the light reaction in green plant chloroplasts. In the green box PS II is shown where water is oxidized at the oxygen evolving complex, in the red box, the reductive part of the light reaction is shown, taking place at PS I where $NAD(P)^+$ is reduced to NAD(P)H by ferredoxin NADP-reductase.

The decrease in pH inside the thylakoid lumen due to water oxidation leads to the dark formation of adenosine triphosphate (ATP) from adenosine diphosphate by ATP-synthase. ATP is the second energy transport molecule and also important for the subsequent dark reactions of photosynthesis, i.e. the fixation of carbon dioxide and the production of carbohydrates. In the chloroplast stroma via the Calvin cycle takes place and so the energy intermediately stored in the NADH, NAD(P)H or ATP molecules is used to reduce CO_2.

Coming from natural photosynthesis to artificial systems that can do the same chemistry:[3] In Figure 3 an example for a PS I model system is shown. First step: assuming NAD^+ or $NAD(P)^+$ as a substrate the related NADH or NAD(P)H forming enzyme-ferredoxin reductase- is exchanged for a hydrogenation catalyst. In a second step the chlorophyll of PS I which acts as photosensitizer is substituted by a similar suitable polypyrrole complex. Further on, the electrons provided by the plastocyanine have to be provided by an easily oxidizable molecule in excess, a sacrificial electron donor.

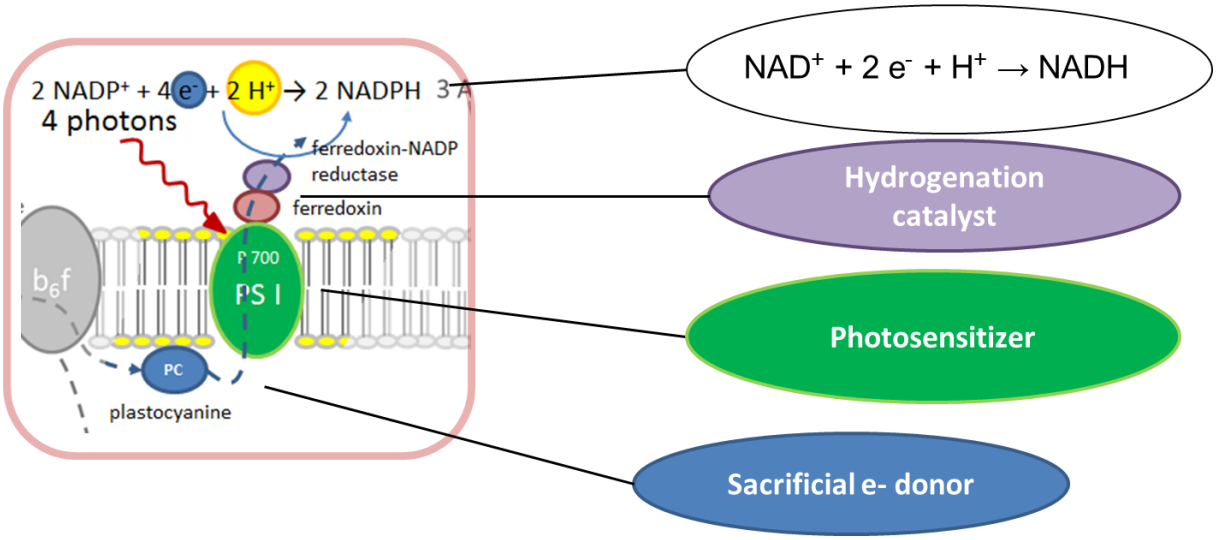

Figure 3 How to build a PS I Model: assuming NAD^+ or $NADP^+$ as a substrate the ferredoxin reductase is exchanged for a hydrogenation catalyst, the chlorophyll of the PS I as a photosensitizer by a similar suitable polypyrrole complex. The electrons provided by the plastocyanine have to be provided by an easily oxidizable molecule, a sacrificial electron donor.[4]

The formation of hydrogen instead of NADH or NAD(P)H, which can be seen as the biological equivalent to hydrogen, shall be taken into account in the context of artificial PS I systems. The reactions forming hydrogen sometimes can be adapted to reduce NADH from NAD^+ instead. At the same time hydrogen formation is a common side reaction in NADH regeneration systems.

Table 1 Redox properties of NAD^+ in aqueous solution compared to protons

Redox pair	E^0 (NHE)	Ref.
$2H^+ + 2e^- \rightarrow H_2$	-0.413 V at pH 7	
$NAD^+ + 2e^- + H^+ \rightarrow$ 1,4-NADH	-0.32 V at pH 7	[5]

The crucial factor in this case is the pH value and, related to this property: the redox potential and the activity of protons in the solution compared to the redox potential and the concentration of NAD^+ (see Table 1). For systems reducing NAD^+ it is necessary to keep the pH value of the solution between 7 and 9 as NADH decomposes at lower pH and NAD^+ is unstable in basic conditions.[6] As can be seen in Table 1 the redox potential of NAD^+ at pH 7 is slightly more positive than the potential necessary for the formation of hydrogen. So an excess of NAD^+ in a regeneration system is a helpful method to supress undesired hydrogen formation.

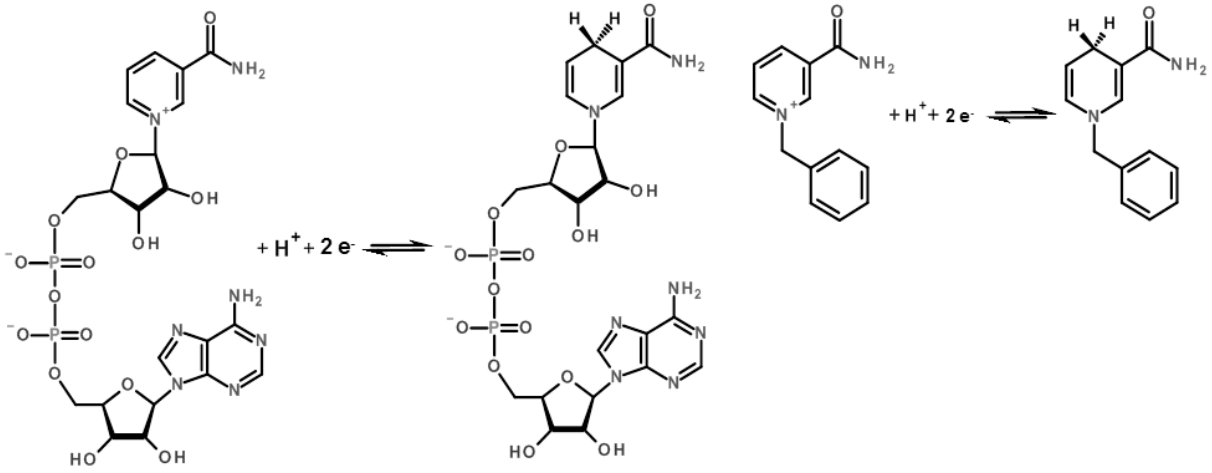

Figure 4 Left side: NAD^+ is reduced to NADH; Right side: the model compound BNA (N-benzyl-3-carbamoyl-pydridinium) is reduced to form BNAH (N-benzyl-1,4-dihydronicotine amide).

The reduction of NAD^+ is obviously stereochemically more demanding than the formation of hydrogen from protons. Only the 1,4-derivative of NADH is enzymatically active and can be

used in subsequent enzymatic reaction steps. As can be seen from Table 1 and especially from Figure 5 it is necessary to catalyse the two electron reduction of NAD^+ to NADH. This has to happen in such a way, that the hydride ends up in the 4-position of the nicotine amide moiety of NADH. The same applies to model compounds similar to **BNA** (N-benzyl-3-carbamoyl-pyridinium).[7–9]

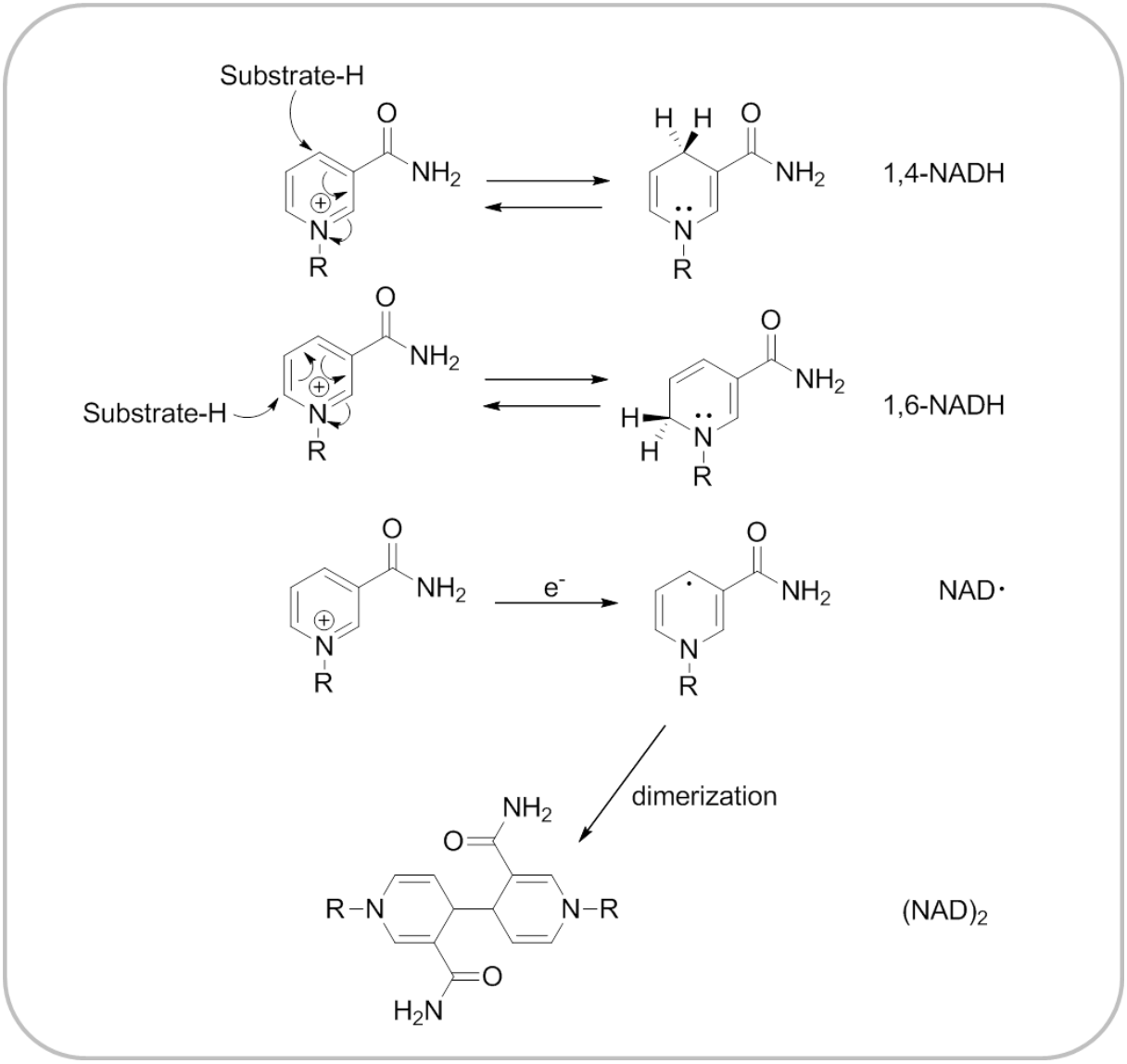

Figure 5 One- and two- electron reduction products and side products in the reduction pathway of NAD^+ and related compounds.[6]

The water soluble rhodium complex $[Rh(H_2O)(bpy)(Cp^*)]^{2+}$ for example can act as a suitable hydride transfer mediator. It provides high selectivity for the formation of the enzymatically active 1,4-isomer of NADH and **BNAH**, the reaction pathway proposed by Lo et al. [7] is shown in Figure 6. Coordination of the carbonyl oxygen of the nicotine amide to the rhodium center facilitates the hydride transfer to the right position to form 1,4-NADH.

The rhodium complex $[Rh(H_2O)(bpy)(Cp^*)]^{2+}$ was initially designed for the photochemical formation of hydrogen on TiO_2[10,11] and further applied for use in chemical and electrochemical cofactor recycling.[12–17]

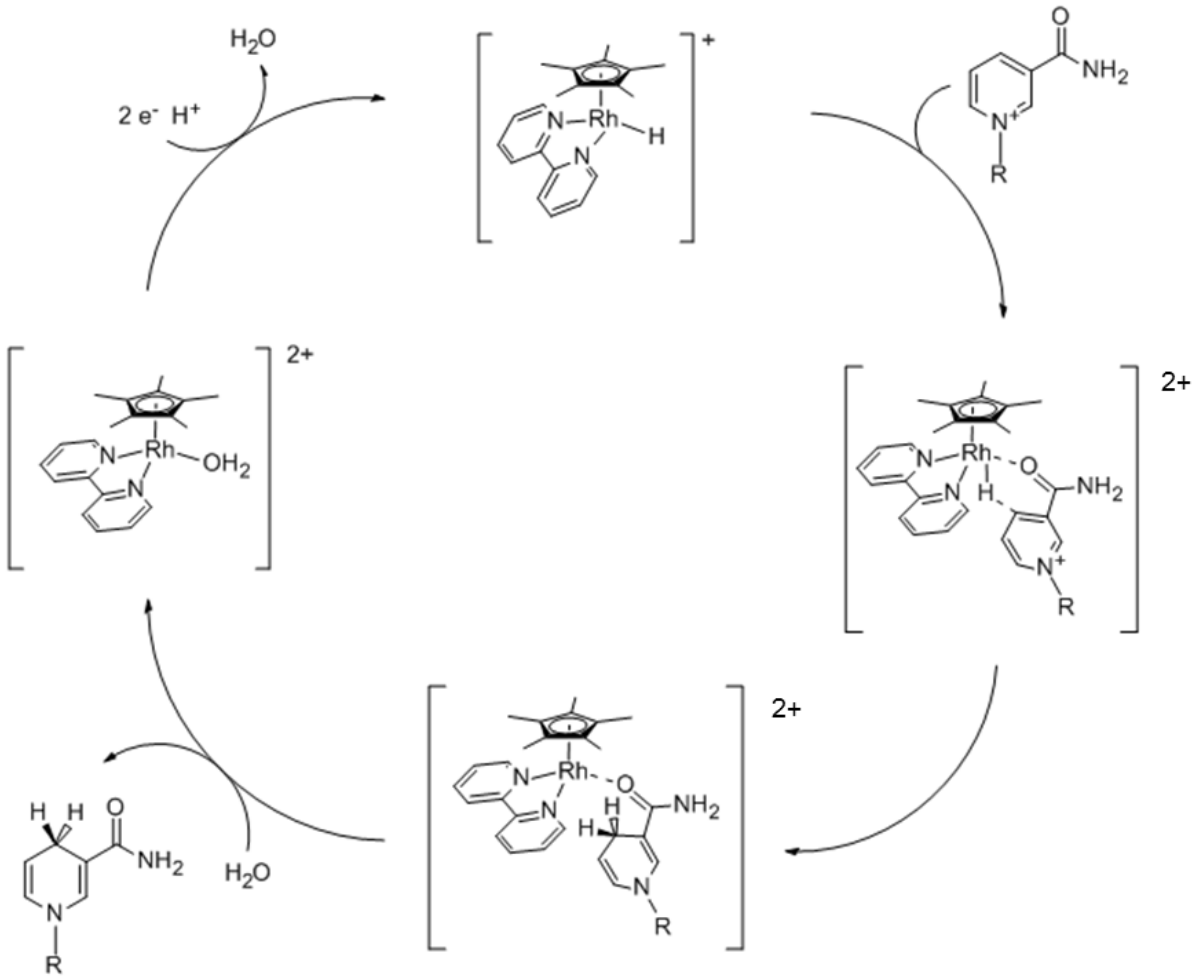

Figure 6 Proposed catalytic cycle for the reduction of NAD^+ and related models catalysed by $[Rh(H_2O)(bpy)(Cp^*)]^{2+}$ generalized from previous work by Lo et al.[7]

Later on, photochemical reduction pathways were investigated. As photosensitizers providing energy for the reduction of NAD^+ by $[Rh(H_2O)(bpy)(Cp^*)]^{2+}$, p-doped TiO_2 nanoparticles[18], SiO_2-supported CdS quantum dots[19], rhodamine laser dyes[20,21] and water soluble zinc porphyrins[22] as well as proflavine[23] have been applied by Park et al.[19–23] and showed good performance in different coupled enzymatic reactions. The lower limit of the light energy in these systems used was around 400-420 nm, which means that these low pass filters were usually applied to the light sources driving the reactions. In a study with proflavine as photosensitizer LEDs were used as light sources and the system also worked with green light, not as good as with blue light though, but no reaction occurred with a red LED as light source.[23]

The most important properties that should be fulfilled by a good sensitizing agent S for a two component system as applied in this work are: high stability, high absorbance of a wide energy range of (visible) light, and also the possibility to harvest light of low energy, i.e. high absorbance in the red region of the solar spectrum. Furthermore a high turnover number (TON)[24] and energy transfer rate to the catalyst applied to drive the hydrogenation reaction. The excited state lifetime and the redox potential of the excited state are crucial points in multicomponent systems that influence the quality of interaction between the redox mediator ($[Rh(H_2O)(bpy)(Cp^*)]^{2+}$) and the photosensitizer molecule.

Due to their excellent stability and their ability to mediate multielectron transfer processes,[25,26,27] tin porphyrins and -chlorins are especially attractive for the sensitization of artificial photosynthetic reactions. Many are based on earth abundant components. Some water-soluble derivatives have been successfully involved in pioneering studies on the photogeneration of hydrogen under visible-light irradiation.[28,29] The photochemical formation of several different hydroporphyrin species is also common under these conditions. [30,31] This chemical behavior depends on the nature of the porphyrin macrocycle as well as the central metal atom which can both influence the redox potential of the photosensitizer.[32]

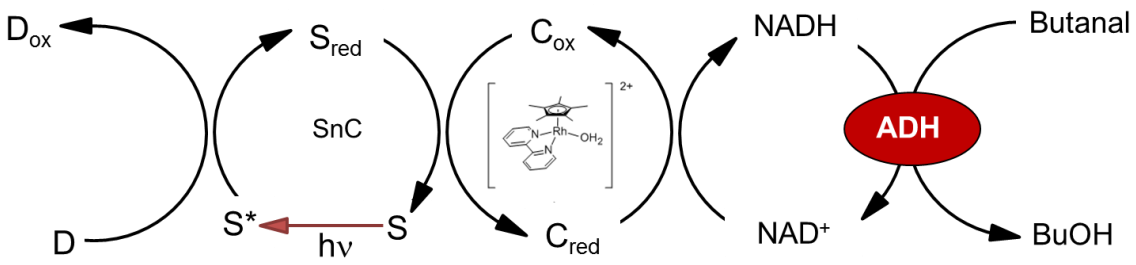

Figure 7 Example for a coupled system with a PS I model and enzymatic reduction of butanal to butanol by means of ADH (alcohol dehydrogenase) as an enzyme that can use NADH as a cofactor[33]

Tin (IV) chlorin exhibits attractive chlorophyll-type spectral properties including an enhanced red light-absorption capability. In Figure 7 an example is shown for how this chlorophyll analogue can become accessible as a photocatalyst for the accumulation of NADH as hydrogen equivalent. This approach allows harvesting of low-energy photons for solar energy conversion and the use of those in subsequent enzymatic reactions. In the example shown the enzymatic reduction of butanal to butanol by means of ADH (alcohol dehydrogenase) as an enzyme using NADH as a cofactor is shown also using $[Rh(H_2O)(bpy)(Cp^*)]^{2+}$ as hydrogenation catalyst.[33]

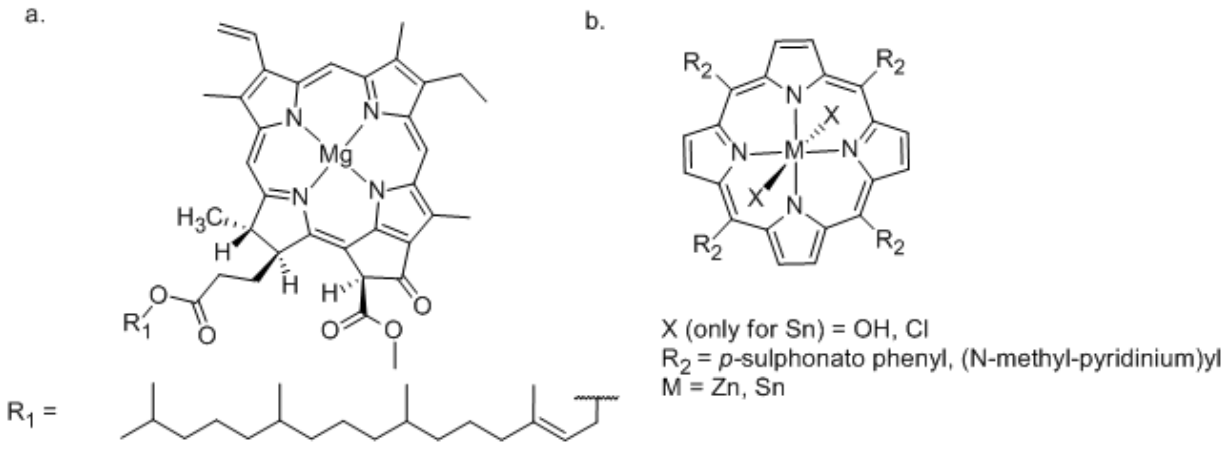

Figure 8 Structural similarities between Chlorophyll a (a.) and zinc (II) or tin (IV) porphyrin an artificial photosensitizer (b.): Zinc (II) porphyrin complexes do not contain axial ligands.

Figure 8 shows the structural similarity between porphyrins applied in artificial systems to natural chlorophyll. Chlorophylls have a chlorin basic structure, which means, that one pyrrole-bond of the macrocycle is saturated, which leads to a red shift in absorbance as compared to the parent porphyrin species. In Figure 9 typical absorbance spectra of the porphyrin and xanthene dye photosensitzers applied in this study are compared to the absorbance spectrum of chlorophyll

b. The natural PS shows much higher absorbance in the lower energy range around 630 nm as compared to the porphyrin sensitizer. Photosensitizers best suited for a system mimicking PS I, besides the properties mentioned above, is also their ability to use red light for the reduction i.e. light with 680 nm or 700 nm, as present in the natural reaction cascade, allowing to harvest low energy photons, which is absolutely necessary to increase the efficiency of solar energy conversion.[34] In Figure 10 the UV-Vis spectra of the Q-band energy region of chlorophyll *b* and tin(IV)-*meso*-tetrakis(*N*-methylpyridinium)-chlorin (**SnC**) are shown for comparison. Chlorophyll *b* is one of the visible-light-harvesting complexes in natural photosynthetic antenna proteins. SnC and chlorophyll *b* show comparable threshold wavelengths at around 660 nm (dashed line).[33]

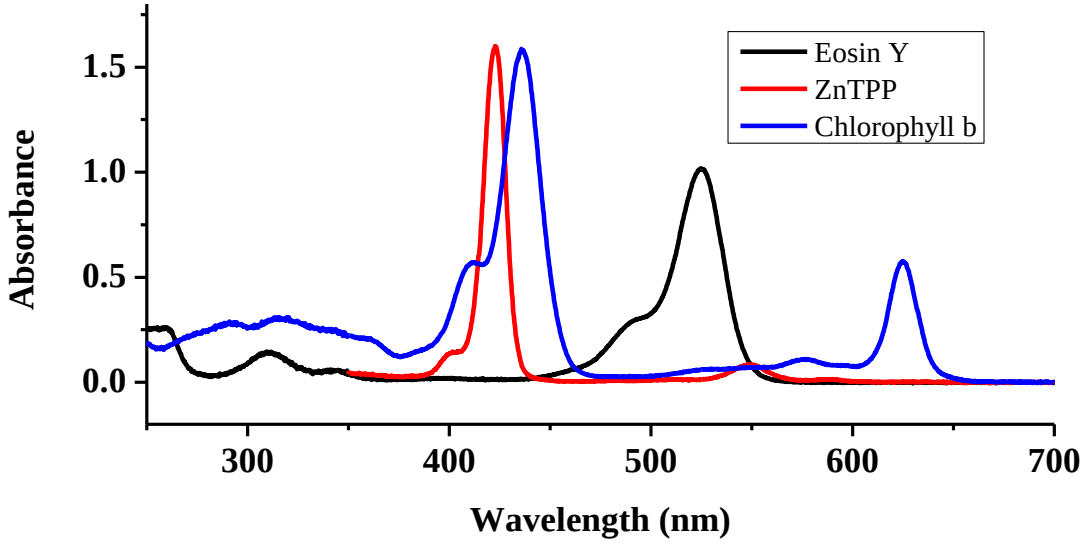

Figure 9 Comparison of the absorbance spectra of porphyrins (example Zinc (II) tetraphenyl porphyrin), eosin Y and chlorophyll b in ethanol solution (data from PhotochemCAD 2.1).[35]

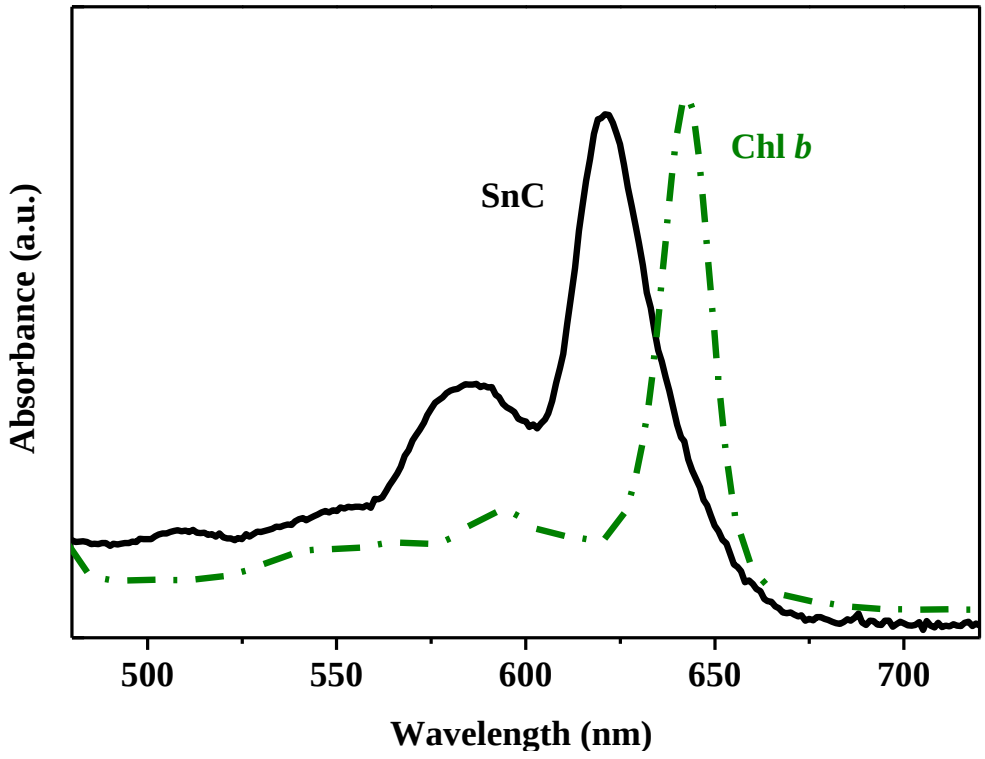

Figure 10 Comparison of the Q-band absorption pattern of the water soluble tin(IV)-*meso*-tetrakis(*N*-methylpyridinium)-chlorin complex SnC (solid line) with the visible-light-harvesting features of native chlorophyll *b* from natural photosynthetic antenna proteins, showing a comparable threshold wavelength at around 660 nm (dashed line).[33]

In the long run, it would be beneficial to be able to combine the porphyrins or related compounds as photosensitizers with a hydrogenation catalyst having a metal centre with a more abundant metal, as rare earth metal complexes are quite expensive for large scale use. This is how cobalt complexes come into play to substitute rhodium based catalysts.

Chlorobis(dimethylglyoximato)(pyridine)cobalt(III) (**CoOxime**) (see Figure 11) and related Co(II)- and Co(III)oxime complexes have shown potential as water reducing catalysts[36,37] in combination with xanthene dyes such as Rose Bengal and Eosin Y[38] or similar xanthene dyes with enhanced excited state lifetime.[39] Acriflavine[40] or porphyrins[41–43] and other metallocomplexes[44] especially ruthenium bipyridyl-complexes[36], have also been applied as photosensitizer in systems for hydrogen evolution by cobaloximes. The first photocatalytic system applying a water soluble cationic zinc porphyrin and

chlorobis(dimethylglyoximato)(pyridine)cobalt(III) for photochemical hydrogen formation was recently reported by Lazarides et al.[45]

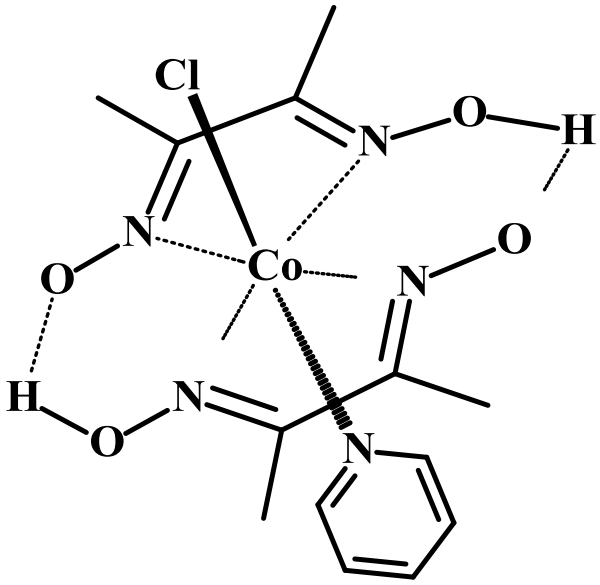

Figure 11 Chemical structure of Chlorobis(dimethylglyoximato)(pyridine)cobalt(III) (CoOxime)

It has been shown by Kim et al.[46] that using Eosin Y as photosensitizer that small amounts of NADH can be formed in an almost purely aqueous system, without addition of any organic solvents besides the sacrificial donor triethanolamine (TEOA). The following investigation which was conducted both experimentally and via literature research analysed the possibilities to combine a metalloporphyrin or -chlorin sensitizer and cobaloxime complexes for the photochemical reduction of redox cofactors.

For the successful reduction of the redox cofactor NAD^+ it is necessary, that the active species of the catalyst has a redox potential more negative than the redox potential of the cofactor and it has to be able to at least provide two electrons at a time, together with a proton, which means it should be able to transfer a hydride in the best case in order to avoid radical formation and dimerization of NAD.[6] At the same time it should be selective to form the enzymatically active 1,4-NADH isomer.[47,48]

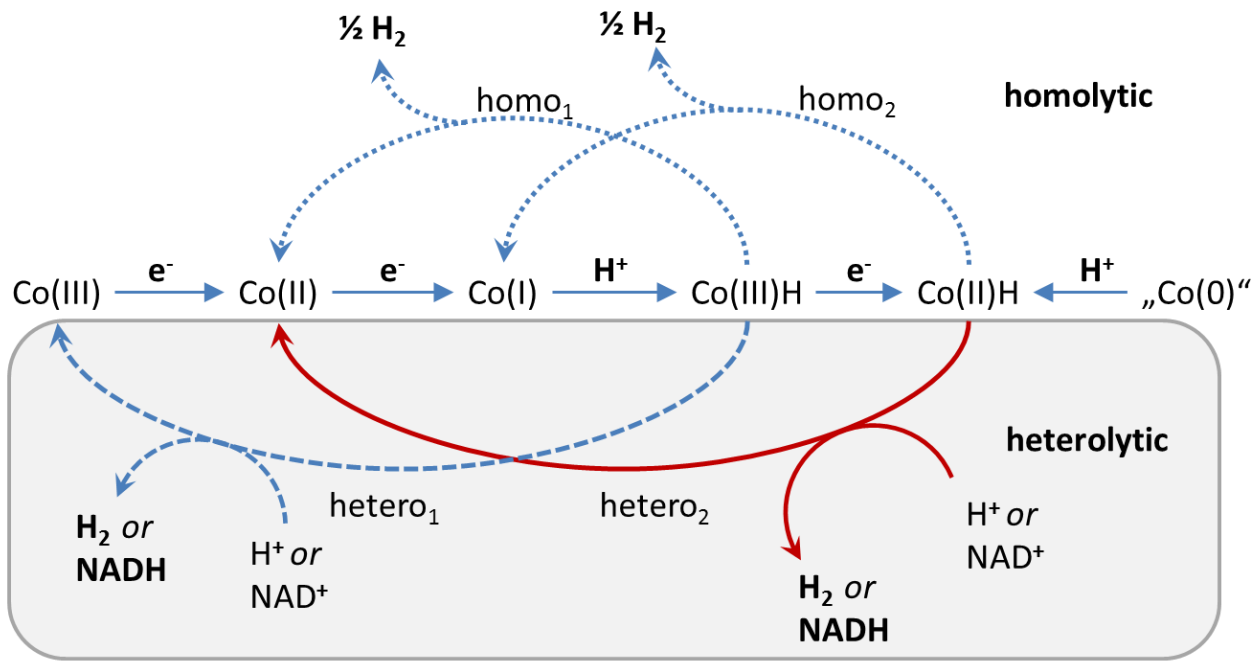

Figure 12 Possible redox reaction pathways for the formation of hydrogen with cobaloxime complexes, adapted from lit.[36] In the grey box the pathways interesting for hydrogenation reactions, and thus for the reduction of NAD^+, are added and highlighted.

In Figure 12 possible hydrogen evolution pathways for cobaloxime complexes are summarized: Starting from the two electron reduction of Co(III) followed by protonation of the Co(I)species to form a Cobalt (III) hydride -Co(III)H. From there, two different hydrogen evolution pathways are possible, involving either homolytic or heterolytic splitting of the cobalt-hydrogen bond. Homolytic pathways are generally favoured, especially at high concentrations of Co(III)H.[49] An excess of strong reductants and low concentrations of Co(III)H under slightly basic conditions however promote the formation of a Co(II)H via reaction of Co(III)H with Co(I), as Gray and coworkers reported.[50] This pathway was also proposed by Lazarides et al. for the formation of hydrogen in their water soluble porphyrin/cobaloxime/TEOA-system[45] and provides the most probable pathway for the reduction of NAD^+ as well because of the similarity of the conditions, although Kim et al. proposed otherwise.[46]

The redox potentials of different cobalt complexes are shown in Table 2. As can be seen from quantum chemical calculations[37], the $Co(dmgBF_2)_2$ has a redox potential for the Co(III)H/ Co(II)H couple slightly more positive than for Co(II)/ Co(I) which lies at -0.30 vs. NHE. This

potential is possibly not reducing enough to drive the reduction of NAD^+ under neutral or slightly basic conditions in aqueous systems. The advantage of this compound is its stability, as the parent cobaloxime chlorobis(dimethylglyoximato)(pyridine)cobalt(III) (**CoOxime**) lacks stability in purely aqueous solution and is therefore mostly used in mixed buffered solvents such as acetonitrile/ water.[38,39,44,51,52]

Table 2 Redox potentials of Cobaloximes in acetonitrile[36]

Cobalt complex	**E^0Co(III)/Co(II)**	**E^0Co(II)/Co(I)**
CoOxime [a]	-0.68 vs. SCE (-0.43 vs. NHE)	-1.13 vs. SCE (-0.88 vs. NHE)
$Co(dmgBF_2)_2$ [b]	0.2 vs. SCE (0.55 vs. NHE)	-0.55 vs. SCE (-0.30 vs. NHE)
E^0Co(II)/Co(I) < E^0Co(III)H/Co(II)H[37,49,50]		

[a] Chlorobis(dimethylglyoximato)(pyridine)cobalt(III); [b] Bis(borondifluorodimethylglyoximate)-cobaltate(II)dimethanolate

Experimental Part

Materials

Tin (IV) meso-tetrakis(N-methylpyridinium) porphyrin hexachloride (**SnP**) was synthesized and characterized according to literature procedures.[53]

Zinc (II) *meso*-tetrakis(N-methylpyridinium) porphyrin tetrachloride (**ZnP**) was prepared according to a modified literature procedure[54] by refluxing 19.8 mg of meso-tetrakis(N-methylpyridinium) porphyrin tetrachloride (Midcentury P.O. Box 217 Posen, IL 60469) with 45.8 mg zinc acetate dihydrate (B&A Allied Chemicals, ≥99.0%) in 20 ml methanol (absolute, anhydrous, Macron Fine Chemicals) at 40°C for 2 h. The reaction was followed by UV-Vis spectroscopy. The solvent was removed and the residual dry product was further dried at high vacuum for 30 min to remove residual solvent. Then the product was dissolved in ultrapure water and used as such for subsequent photolysis experiments or further purified by size exclusion chromatography on Sephadex-20 with ultrapure water as eluent.

Zinc (II) *meso*-tetrasulphonatophenyl porphyrin tetrachloride (**ZnTSPP**) was prepared according to a modified literature procedure[54] by refluxing 23.8 mg of free base sodium-*meso*-tetrasulphonatophenyl porphyrin (Strem Chemicals) with 4.2 mg zinc acetate dihydrate (B&A Allied Chemicals, ≥99.0%) in 20 ml methanol (absolute, anhydrous, Macron Fine Chemicals) at 50°C for 2 h. The reaction was followed by UV-Vis Spectroscopy. The solvent was removed under reduced pressure and the product was further dried at high vacuum to remove residual solvent. Then the product was dissolved in ultrapure water and used as such for subsequent photolysis experiments.

Ruthenium-trisbipyridine ($Ru(bpy)_3Cl_2 \cdot H_2O$) was purchased from Strem Chemicals and used as is.

The cobaloxime complex chlorobis(dimethylglyoximato)(pyridine)cobalt(III) (**CoOxime**) was synthesized in the following way: Dimethylglyoxime was added to a solution of $CoCl_2.6H_2O$ (5.0 g, 21 mmol) in 100 ml of 95% ethanol, followed by pyridine (3.44 g, 43 mmol). The mixture was vigorously aerated for 20 min with occasional swirling. Then 5 ml of water were added and the brown dispersion was aerated for another 1.5 h. The product was collected by centrifugation, repeatedly washed with water and air-dried.

Bis(borondifluorodimethylglyoximate)cobaltate(II)dimethanolate (**$Co(dmgBF_2)_2$**) was obtained by in house synthesis from Etsuko Fujita.

Nicotineamide adenine dinucleotide hydrate from yeast (**NAD^+**) and **NADH** were purchased from Aldrich.

N-benzyl-3-carbamoyl-pyridinium hexafluorophosphate (**BNA**) was provided by Dmitry Polyansky and Yasuo Matsubara.

Solvents

All buffer solutions were prepared with ultrapure water (> 18.2 MΩ). Acetonitrile (ACN) (HPLC grade) and triethanolamine (TEOA) (puriss. p.a. ≥ 99%) were purchased from Sigma-Aldrich. Methanol (abs., anhydrous) was obtained from Macron Fine Chemicals.

Triethanolamine/sodium phosphate buffer solutions were prepared by addition of a suitable amount of TEOA to a 0.1 M solution of anhydrous dibasic sodium phosphate (J.T. Baker, 99.9%) and sodium phosphate monobasic monohydrate (Sigma-Aldrich ≥99%) and adjustment of the pH value by addition of hydrochloric acid (37%, Sigma Aldrich). TEOA solutions with a defined pH were prepared by dilution of a suitable amount of TEOA with ultrapure water and adjustment of the pH value by addition of hydrochloric acid (37%, Sigma Aldrich).

Electrolyte solutions for electrochemistry were prepared by dissolution of 5.165 g tetrabutylammonium hexafluorophosphate (Fluka, ≥ 98%) in 130 ml acetonitrile which was pre-dried using active alumina.

Instrumentation

Photolysis

UV-Vis Spectrometer: Optical Fibre Spectrometer Ocean Optics USB2000+ with DT-Mini-2 light source and SpectraSuite 5.1 Software, Agilent 8453 diode array spectrophotometer and HP 8452A diode array spectrophotometer.

Photoluminescence

For Photoluminescence measurements a PTI Fluorimeter with a LPS-220B Arc lamp power supply, 75 W Xe-lamp, FeliX 1.42a Software and Time Master Control module was used.

GC

Gas chromatography was done with an Agilent 6890N GC equipped with a thermal conductivity detector. The ChemStation Software Re.A.10.01 was used for data recording and analysis.

HPLC

The HPLC system consisted of a surveyor PDA detector, and the XCalibur Software. The column was a TSKgel ODS-100V 5µm, P/N 21455.

Electrochemistry

Cyclic voltammetry was performed using a CH Instruments Electrochemical Workstation with CHI 11.13 Software and BASi MF-2012 Glassy Carbon Electrode (GCE) (3.0 mm dia.) as working- and a MF-2013 Platinum Electrode (PTE) (1.6 mm dia.) as counter electrode. The non-aqueous reference electrode (MF-2062) with a silver wire, 0.1 M tetrabutylammonium hexafluorophosphate ($TBAPF_6$) and $AgNO_3$ was separated from the sample compartment using a PEEK Reference Electrode Retainer (MR-3068).

Bulk electrolysis was done using a glassy carbon electrode (6 mm diameter). The non-aqueous reference electrode (MF-2062) with a silver wire, $AgNO_3$ and 0.1 M $TBAPF_6$ was separated from the sample compartment using a PEEK Reference Electrode Retainer (MR-3068). A simple platinum wire was used as counter electrode.

Spectroelectrochemistry was performed with a HP 8452 diode array spectrophotometer and a BASi 100B Potentiostat connected to a computer running the BASi 100W software. As a quasi-reference electrode $Ag/AgNO_3$/0.6 M $TBAPF_6$ in acetonitrile was used in a separator containing 0.1 M $TBAPF_6$ in acetonitrile. The working electrode was glass/ITO and connected to Al foil with Parafilm and the counter electrode was a simple Pt wire.

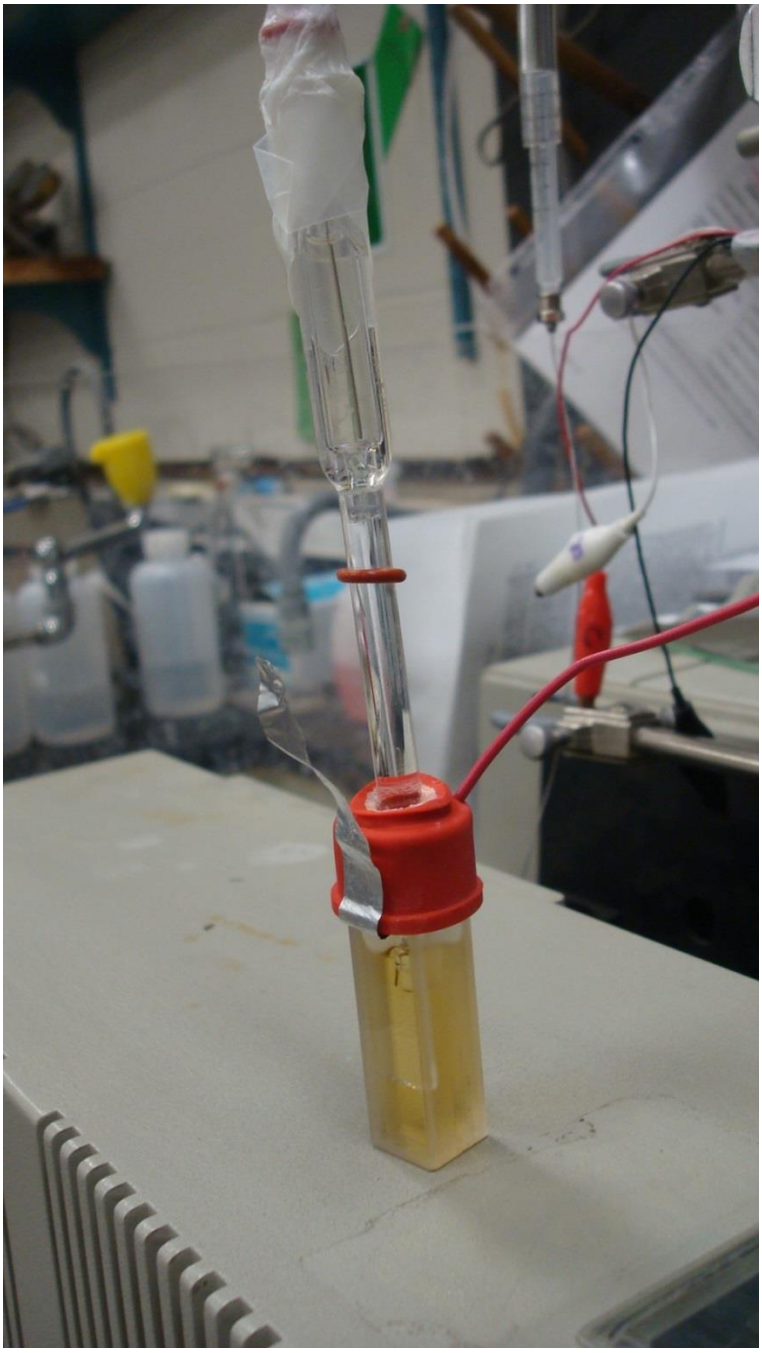

Figure 13 Spectroelectrochemical cell: 1 cm quartz cuvette, ITO working electrode, Pt counter electrode and Ag/ AgCl reference electrode in a reference electrode retainer

Methods

UV-Vis spectra were taken in different time intervals throughout all photolysis experiments. NADH has a distinct absorbance band at 340 nm with $\varepsilon = 6300\ cm^{-1}\ mol^{-1}\ l$,[55] so quantification of the photolysis product by optical spectroscopy is usually straight forward using Lambert-Beer's Law. The cobalt(II) species in the solution has a strong absorbance at 450 nm and the corresponding Co(I) species shows a broad absorbance in the range from 550 to 600 nm, which can be used to determine how fast the reaction is proceeding in terms of formation of the actual water reducing species.[38] Additionally porphyrins and hydroporphyrins can be observed via UV-Vis due to changes in the absorbance spectra upon reduction of the porphyrin macrocycle.[56,57]

For photoluminescence measurements with the PTI the slits are given in parentheses (entrance slit width in nm/ exit slit width in nm) for experiments in the figure caption. NADH has a broad fluorescence between about 420 and 550 nm with a fluorescence maximum at 470 nm,[55] which can be detected by photoluminescence measurements upon excitation at the absorbance maximum at 340 nm under most circumstances, if other components in the solution do not or only weakly absorb at these particular wavelengths. In Figure 14 an example is shown for this method. A photolysis sample containing 7.5 μM tin (IV) tetrakis-(*N*-methyl-pyridiniumyl)chlorin (**SnC**); 1 mM NAD^+; 15 w/v% TEOA and 7.7×10^{-5} M $[RhCp^*(bpy)H_2O]^{2+}$ was irradiated with a 150 W Xenon light source with a 610 nm cut-off-filter. Time dependent emission spectra were recorded. In this system the absorbance of both the hydrogenation catalyst as well as the absorption of the porphyrin photosensitzers do not hinder the observation of the reduced cofactor absorbance and emission. As can be seen later this is very much different for the solution containing cobaloxime and/or eosin Y - especially in higher concentrations. Here a chromatographic detection method had to be installed.

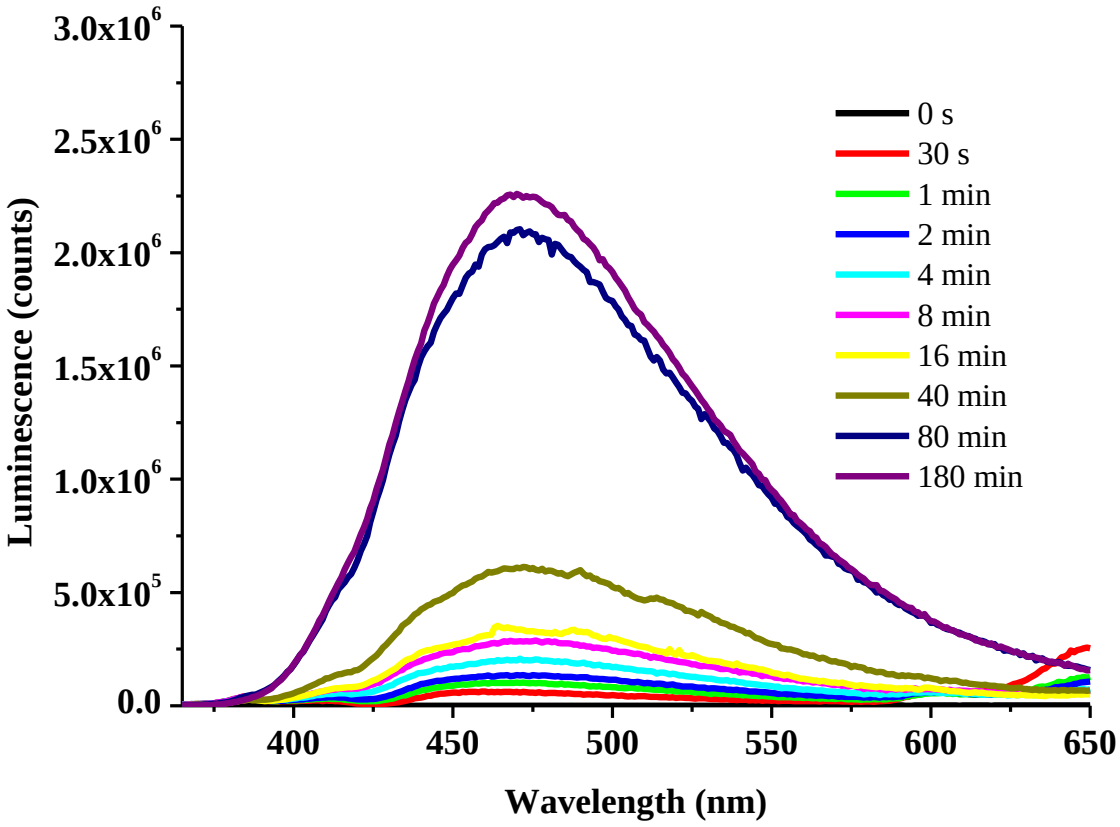

Figure 14 Luminescence spectra of a solution containing: 7.5 µM SnC; 1 mM NAD^+; 15 w/v% TEOA and 7.7 ×10^{-5} M $[RhCp^*(bpy)H_2O]^{2+}$ under Ar in 0.1 M phosphate buffer pH 8.8; irradiated with a 150 W Xenon light source with a 610 nm cut-off-filter. Increasing luminescence upon excitation at 340 nm exhibiting a maximum at λ_{max} = 470 nm (ϕ= 0.02) indicates reduction of NAD^+ to NADH.[33]

Photolysis experiments were performed in quartz glass cuvettes equipped with a screw cap and a septum to remove gas samples from the head space of the sample solution if not otherwise mentioned. Samples were purged with Ar for 20 min prior to any photolysis experiment to remove oxygen if not stated differently. In order to cut off of high energy light suitable glass low pass filters additional to a $CuSO_4$-IR filter and a heat absorber filter HA-20. Transmission spectra of all filters used are shown in Figure 15 for later reference throughout this report. All solutions were kept at 25°C while irradiated and stirred with a small magnetic stirrer at 1400 rpm. For special purposes a gas tight fluorescence cuvette with Svagelock joint and tubing to connect to the sample loop of the GC was used.

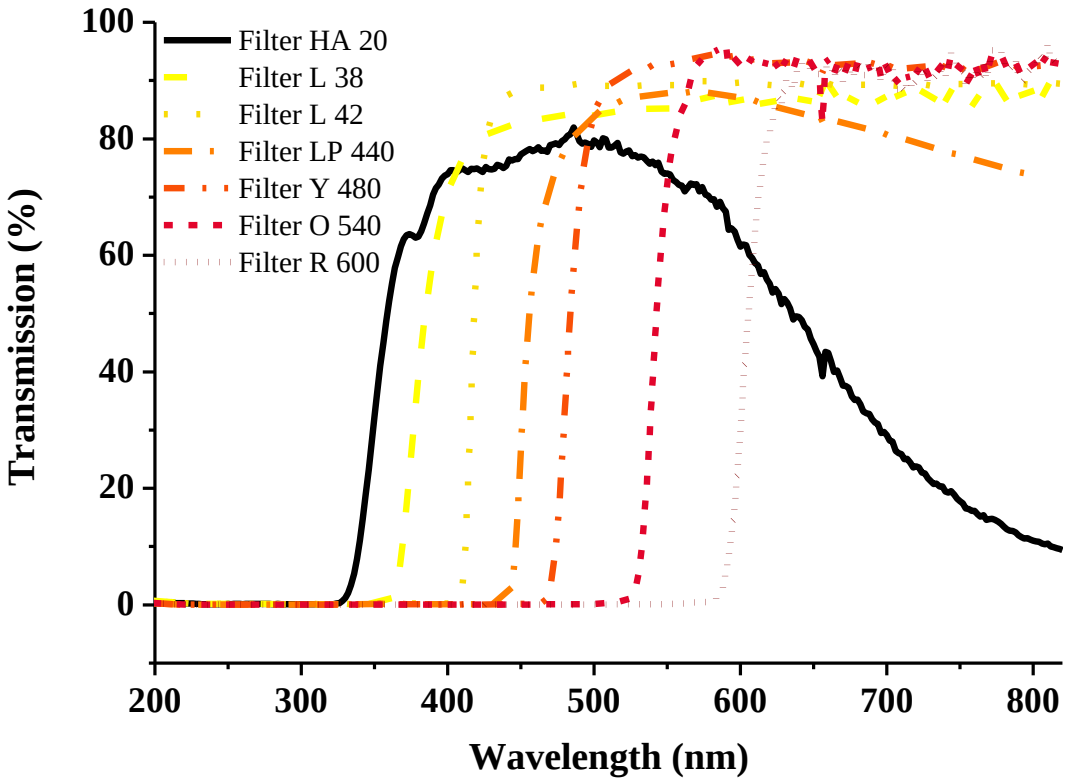

Figure 15 Transmission spectra of the glass filters used in photolysis experiments.

For some experiments a small gas pump (Spectra Physics) was used to purge the solution with ambient air.

The method for the Agilent 6890N gas chromatograph applied was 40°C isothermal flow (18 ml min^{-1}) using argon as carrier gas. The injection volume was 100 µl if not otherwise mentioned, a thermal conductivity detector (TCD) was used for detection. Quantification of the gases was done by external calibration.

For detection of **BNA/ BNAH** the mobile phase was 70% methanol in water with 20mM sodium phosphate. For the separation of solutions containing NAD^+ and NADH the mobile phase was 100 mM sodium phosphate buffer pH 7 containing 1 mM dihydrogen disodium ethylene diamine tetraacetate (EDTA) with 10% methanol. Gradient elution was not necessary. The HPLC flow rate was 0.6 ml min^{-1} for all measurements.

Electrochemical measurements were performed in dry acetonitrile containing 0.1 M tetrabutylammonium hexafluorophosphate ($TBAPF_6$) which was purged with argon gas (pre-saturated with ACN) to remove oxygen. During the measurements argon was used as blanket gas above the sample solution in the cell. As the solution was non-aqueous and a quasi-reference electrode was used, the electrode potential of the working electrode was calibrated using the ferrocene/ferrocenium redox couple. The formal electrode potential of Fc/Fc^+ is $E^{0'}$= 0.40 V vs. SCE[58] and for the SCE a value of 0.241 mV against NHE[59] was assumed for calculations. The potential values in the following graphs are given against NHE.

Bulk electrolysis were performed in dry acetonitrile containing 0.1 M tetrabutylammonium hexafluorophosphate ($TBAPF_6$) which was purged with argon gas (pre-saturated with ACN) to remove oxygen. During the measurements argon was used as blanket gas above the sample solution in the cell and the solution was vigorously stirred with a magnetic stirrer. As a quasi-reference electrode was used in the non-aqueous system, the electrode potential of the working electrode was calibrated using the ferrocene/ferrocenium redox couple. The formal electrode potential of Fc/Fc^+ with $E^{0'}$= 0.641 V vs. NHE[58,59] was assumed for calculations.

Spectroelectrochemistry was done in volumes of 3 ml dry acetonitrile containing 0.1 M tetrabutylammonium hexafluorophosphate ($TBAPF_6$) which was purged with argon gas (pre-saturated with ACN) to remove oxygen. During the measurements argon was used as blanket gas above the sample solution in the cell and the solution. During controlled potential electrolysis UV-Vis spectra were recorded in specified time intervals with the photodiode array spectrometer. After finishing all measurements ferrocene was added to the solution and a cyclic voltammogram was recorded to determine the exact electrolysis potential. The formal electrode potential of Fc/Fc^+ with $E^{0'}$= 0.641 V vs. NHE[58,59] was assumed for calculations.

Results and Discussion

The normalized optical absorbance spectra of the investigated coordination compounds chlorobis(dimethylglyoximato)(pyridine)cobalt(III) (**CoOxime**) and tin (IV) meso-tetrakis(N-methylpyridinium) porphyrin hexachloride (**SnP**) under the mostly applied reaction conditions are given in Figure 16 for later reference. Especially the tin (IV) porphyrin can exchange the initial axial chloro-ligands to water or hydroxide and thus exhibits pH-dependent absorbance properties.[27] The absorbance maximum of the B-band of the porphyrin can be found at 423 nm, the absorbance of the Q-bands at 555 and 593 nm. The cobaloxime complex shows strong absorbance in the UV-range with a maximum at 246 nm and a shoulder at about 290 nm and very weak absorbance at wavelengths ≥ 400 nm.

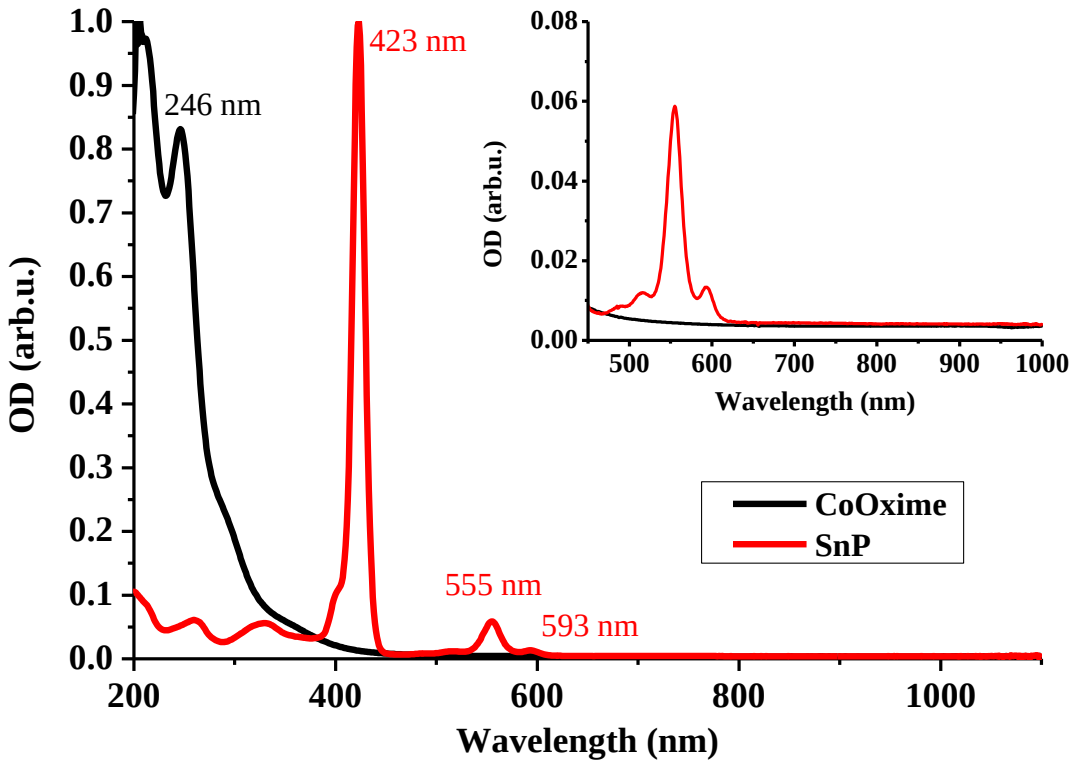

Figure 16 Normalized UV-Vis spectra of chlorobis(dimethylglyoximato)(pyridine)cobalt(III) (CoOxime)-black solid line- and tin (IV) meso-tetrakis(N-methylpyridinium) porphyrin hexachloride (SnP)- red dashed line- in 0.1 M sodium phosphate buffer pH = 7.Inset: Magnification of the Q-band region from 450 to 1000 nm.

Photolysis Experiments

Photolysis experiments were performed using 4 different photosensitizers:

- Eosin Y (as a benchmark sensitizer),[38]
- Tin (IV) *meso*-tetrakis(N-methylpyridinium) porphyrin hexachloride (**SnP**) and
- Zinc (II) *meso*-tetrakis(N-methylpyridinium) porphyrin tetrachloride (**ZnP**).[45]
- Zinc (II) *meso*-tetra-*p*-sulfonatophenyl porphyrin **(ZnTSPP)**
- Ruthenium-*tris*-bipyridine ($Ru(bpy)_3^{2+}$)
- Additional experiments with Tin (IV) meso-tetrakis(N-methylpyridinium) chlorin (**SnC**) were performed, which was obtained via irradiation of the parent porphyrin compound under constant purging of the sample with ambient air[33] previous to photolysis experiments.

As a measure for the quality of interaction between the porphyrin sensitizer and the cobaloxime complex the formation of hydrogen analogous to Lazarides et al.[38,45] has been tested. Some of the photolysis results are summarized in Table 4 in the appendix.

Eosin Y as sensitizer

The excited state redox potential for the oxidation of eosin Y gives around -1.11 V of reducing power, so the cobaloxime can oxidatively quench this state.[44,60]

Irradiation of a sample containing eosin Y, cobaloxime and NAD^+ in with a low pass filter at 420 nm (L-42) and HA 20 similar to the literature[46] with EY:CoOx = 10: 1.2 lead to formation of NADH which can also be detected by HPLC. The sample contained 1 mM eosin Y, 0.18 mM **CoOxime** and 0.75 mM NAD^+ in 0.2 M TEOA/0.1 M sodium phosphate pH 7. Simple detection of NADH via UV-Vis and luminescence measurement was not applicable due to high overall absorption of the sample at the detection wavelength of 340 nm.

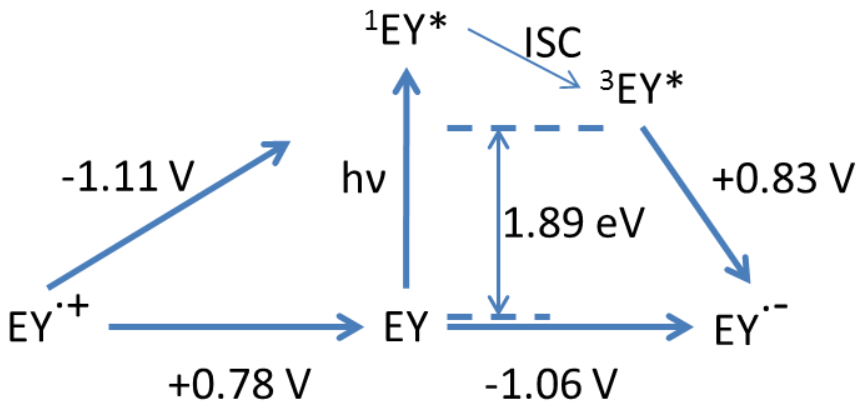

Figure 17 Energy diagram for the excited state redox potential of eosin Y[60] the redox potential

With a turnover number after 1 h eosin Y of 0.75 and a TN for the **CoOxime** of 4 almost 100% conversion of NAD^+ to NADH has been achieved.

Additional GC measurements also show significant amounts of hydrogen formed as side product to the formation of NADH.

Without cobaloxime in the solution no NADH can be detected, and the solution is bleached within 10 min of irradiation.

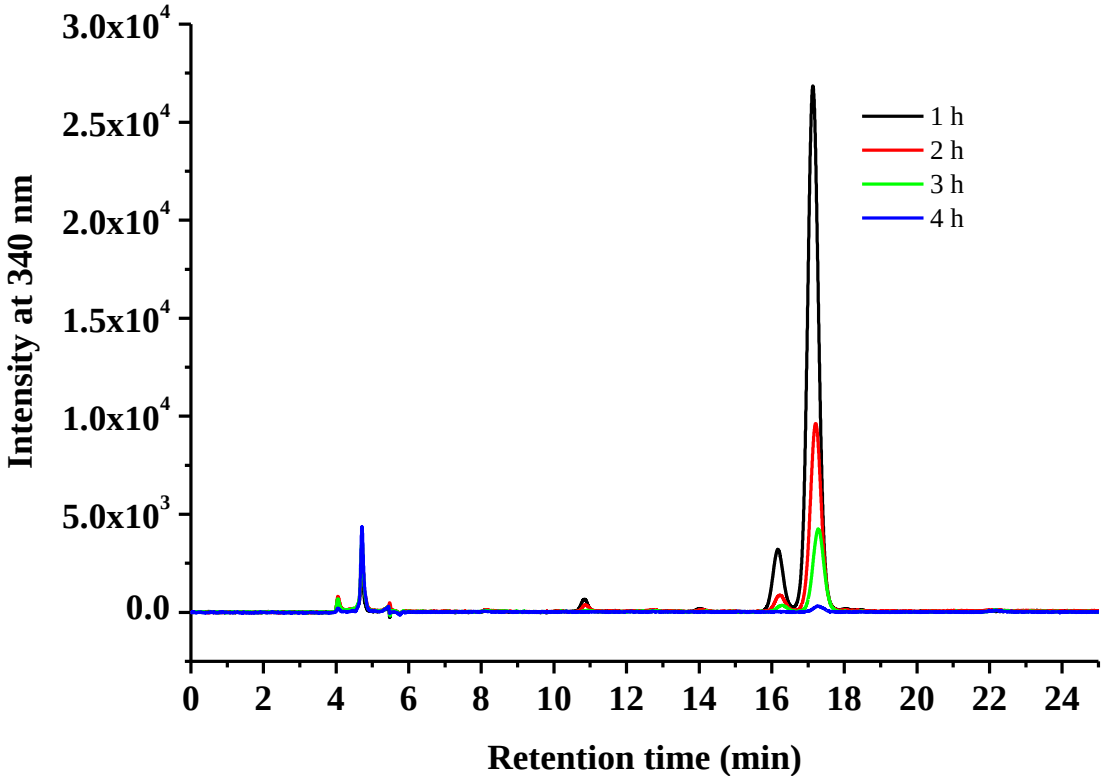

Figure 18 HPLC traces after 1,2,3 and 4 h of irradiation of a sample containing eosin Y as a photosensitizer with cobaloxime with a ratio of EY: CoOx = 10: 1.2. TN (EY): 0.75 TN (CoOx): 4 100% conversion of NAD^+ to NADH

NADH can be seen in the HPLC-chromatogram (Figure 18) and in the UV-Vis spectrum of the HPLC signal at a retention time of 17.35 which can be attributed to the reduced cofactor (Figure 19).

Prolonged irradiation leads to bleaching of the system and presumably further reduction of the cofactor and thus to a decay of the formed NADH. This is especially visible in Figure 20 where the calculated NADH concentration from the HPLC data is plotted versus time.

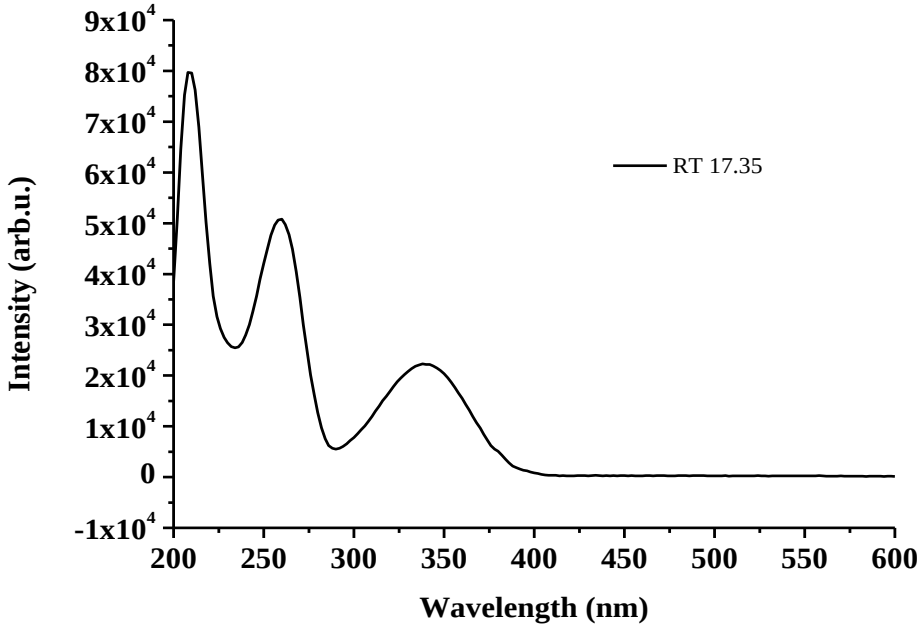

Figure 19 UV-Vis spectrum of the HPLC signal at 17.35 min after 1h of irradiation of a sample containing eosin Y, NAD^+ and CoOxime in a TEOA/sodium phosphate buffer pH 7.

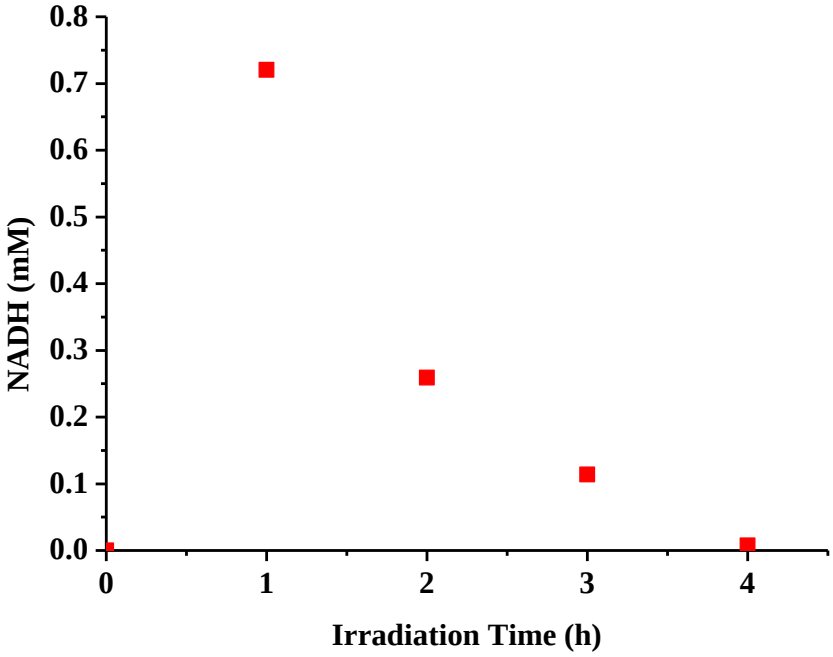

Figure 20 Time course of the photochemical formation of NADH in a buffered solution containing eosin Y, NAD^+, CoOxime and TEOA. Initially formed NADH presumably decays or gets further reduced due to prolonged irradiation of the photochemical system.

SnP as photosensitizer

Figure 21 depicts a UV-Vis spectrum of a typical sample for a photolysis experiment with **SnP** and **CoOxime** in a buffer system with ACN/water containing TEOA as sacrificial donor. The graph shows the first 3 minutes of the photolysis in which spectra were recorded every 10s. The formation of the tin(IV) phlorin can already be observed after 10s of irradiation with $\lambda_{irr} \geq 420$ nm by observation of the B-band bleaching and the formation of new absorbance bands at 750 nm and 830 nm which mostly correspond to the porphyrin radical anion and the phlorin respectively.[56] Prolonged irradiation of the sample as shown in Figure 22 leads to bleaching of the photosensitizer in the photolysis solution, the baseline shifts and after about 300 minutes significant amounts of chlorin are formed as can be seen by increasing absorbance around 623 nm.

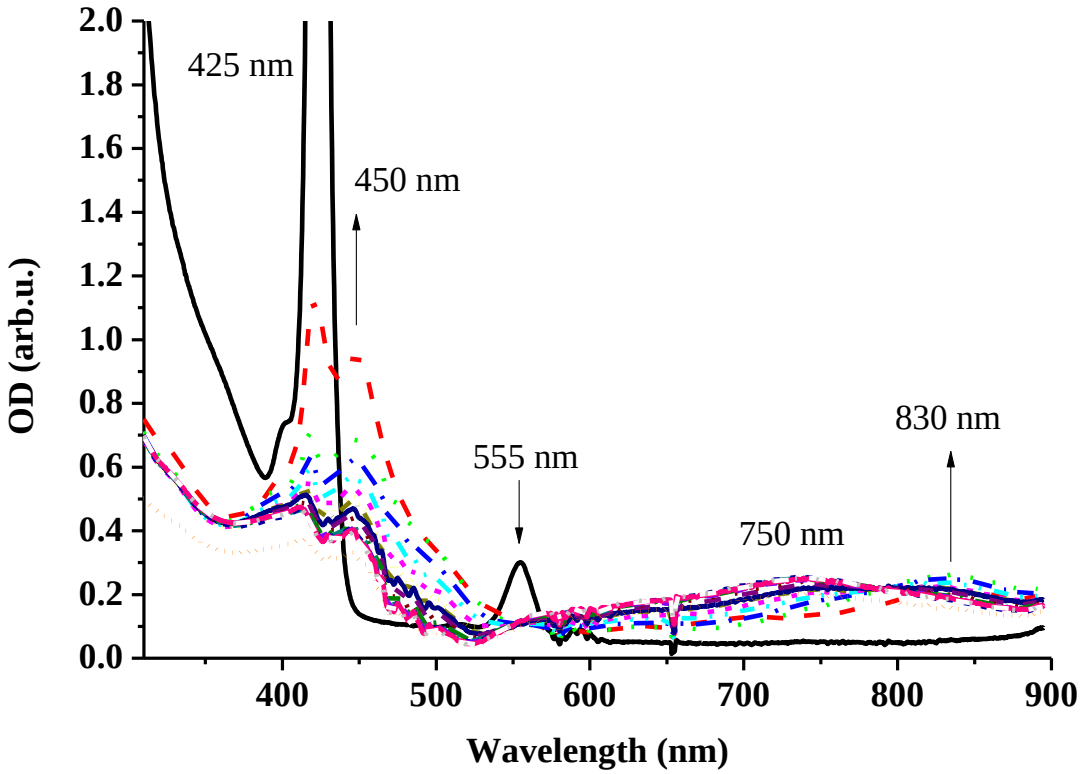

Figure 21 Optical Changes in the first 3 min of the photolysis of SnP (22 µM) and CoOxime (400 µM) in ACN/0.2 M TEOA with 0.1 M sodium phosphate in water pH=7 1:1 irradiated at $\lambda_{irr} \geq 420$ nm, spectra were recorded every 10s.

Samples taken from the headspace of the reaction solution were analysed by GC and the ratio between hydrogen formed and **SnP** of a sample containing **SnP** (22 µM) and **CoOxime** (400 µM) in ACN/0.2 M TEOA with 0.1 M sodium phosphate in water pH=7 1:1 irradiated at $\lambda_{irr} \geq 420$ nm can be seen in Figure 23. The maximum TN for the **SnP** photosensitizer in this experiment was ~5.5 after approximately 400 min.

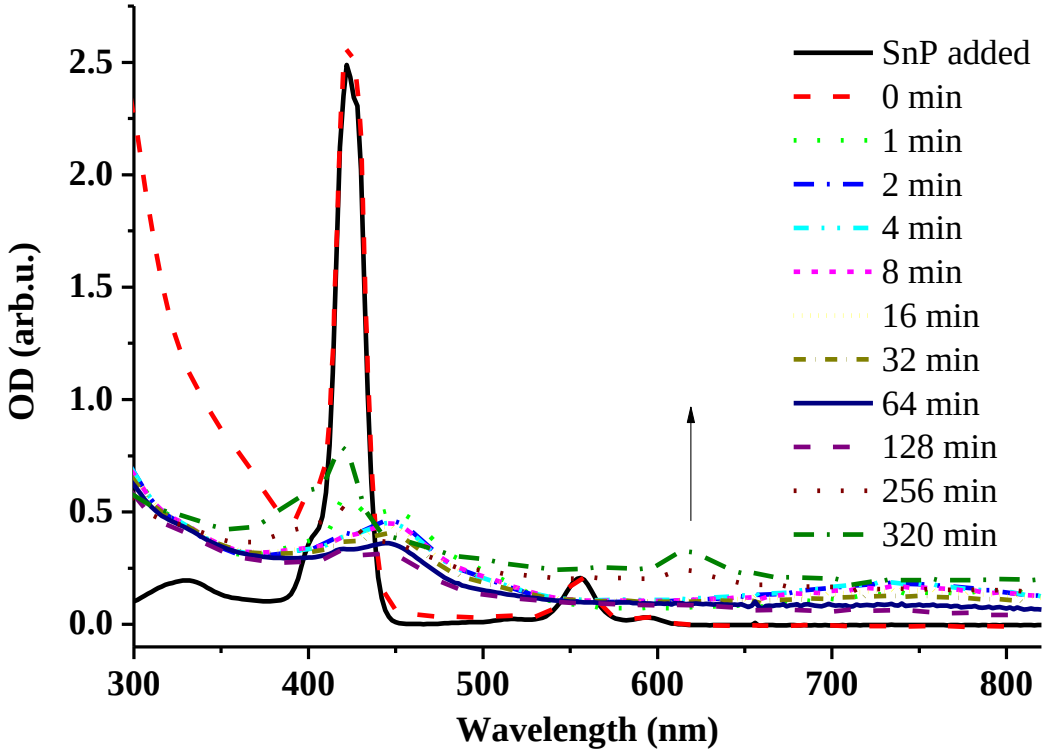

Figure 22 UV-Vis spectrum of a solution containing SnP (22 µM) and CoOxime (400 µM) in ACN/0.2 M TEOA with 0.1 M sodium phosphate in water pH=7 1:1 irradiated at $\lambda_{irr} \geq 420$ nm.

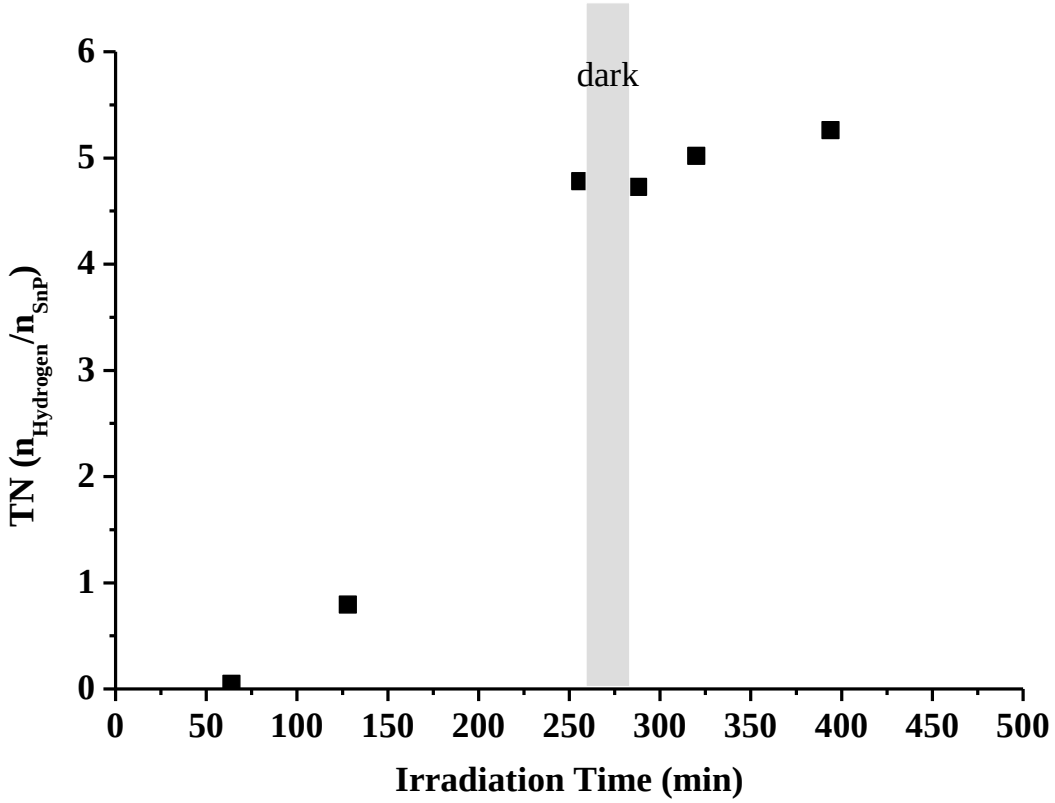

Figure 23 Ratio between hydrogen formed and SnP in the sample containing SnP (22 µM) and CoOxime (400 µM) in ACN/0.2 M TEOA with 0.1 M sodium phosphate in water pH=7 1:1 irradiated at $\lambda_{irr} \geq 420$ nm;

Figure 24 shows the optical absorbance spectra of a solution containing **SnP** (22 µM) and **CoOxime** (400 µM) in 0.2 M TEOA with 0.1 M sodium phosphate in water pH=7 irradiated at $\lambda_{irr} \geq 420$ nm. In this purely aqueous system the amount of hydrogen formed after 450 min (Figure 25) is about twice the amount found in the sample using ACN/water as solvent. The overall concentration of TEOA was also twice as high, which has to be taken into account upon evaluation of this result.

Photoluminescence emission (λ_{exc}=340 nm) and excitation spectra (($\lambda_{meas.}$=460 nm) after different periods of irradiation time of a sample solution containing **SnP** (22 µM) and **CoOxime** (400 µM) in 0.2 M TEOA with 0.1 M sodium phosphate in water pH=7 irradiated at $\lambda_{irr} \geq 420$ nm; slit (5/5) can be seen in Figure 26.The spectrum shown in bold lines was recorded after a photolysis time of 400 min and purging of the solution with air to oxidize Co(II) compounds in the solution in order to minimize their interference with the NADH emission. The sample shows weak emission with a maximum at 460 nm. The corresponding excitation spectrum shows a small intensity

maximum at 360 nm which can be a hint for possible NADH formation according to related literature[46], but there is additional proof (UV-Vis absorbance or coupled enzymatic process) needed.

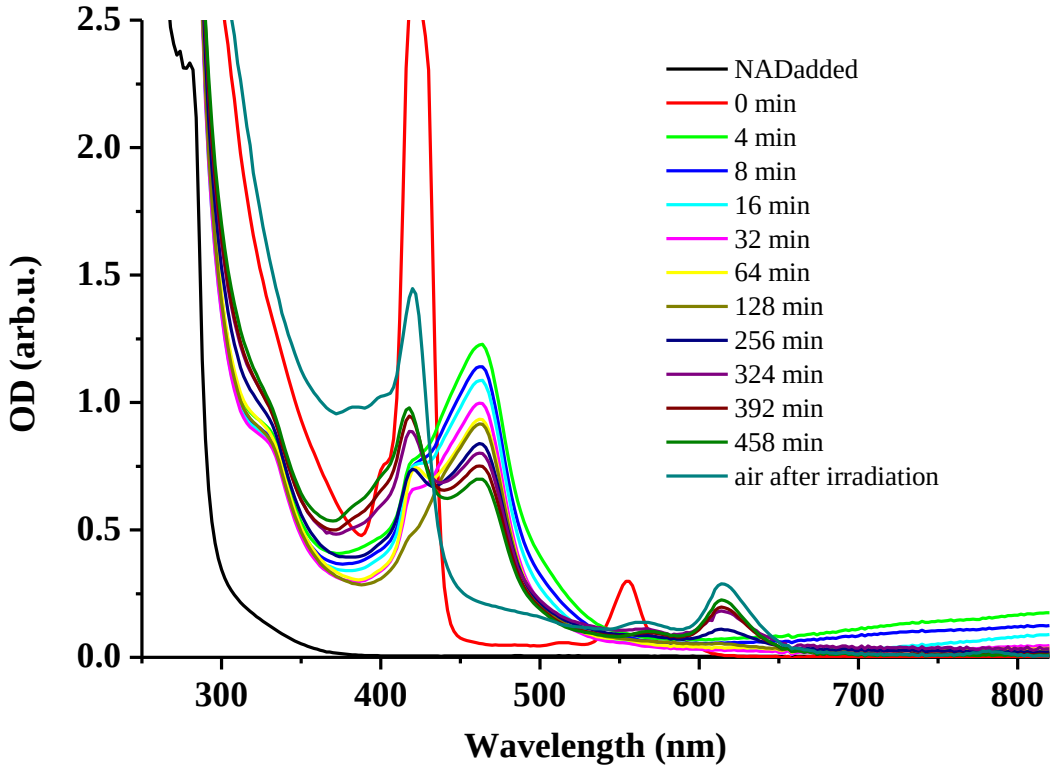

Figure 24 UV-Vis spectrum of a solution containing SnP (22 µM) and CoOxime (400 µM) in 0.2 M TEOA with 0.1 M sodium phosphate in water pH=7 irradiated at $\lambda_{irr} \geq 420$ nm.

In following experiments also HPLC analysis of the sample solution was done, but no detectable amount of NADH could be found in photolysis samples containing NAD^+, **SnP** and cobaloxime, traces of hydrogen however could be found in all samples.

Also in this experiment after a photolysis time of 250 minutes tin(IV)chlorin **SnC** is formed in the solution.

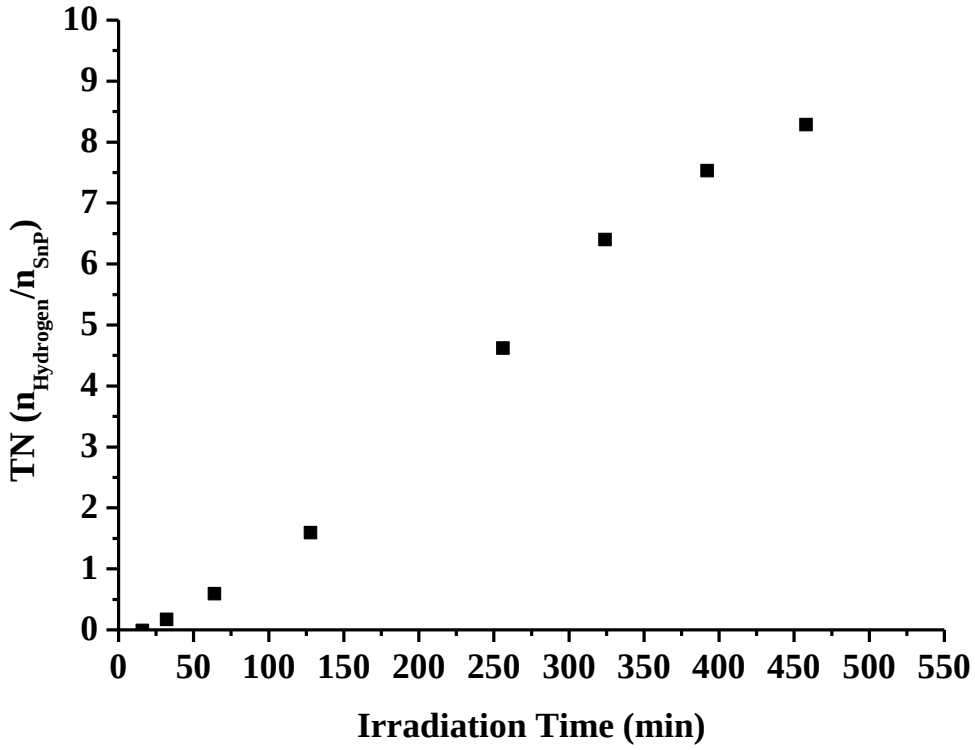

Figure 25 Ratio between hydrogen formed and amount of photosensitizer SnP in the sample containing SnP (22 µM) and CoOxime (400 µM) and NAD^+ in 0.2 M TEOA with 0.1 M sodium phosphate in water pH =7 irradiated at $\lambda_{irr} \geq 420$ nm.

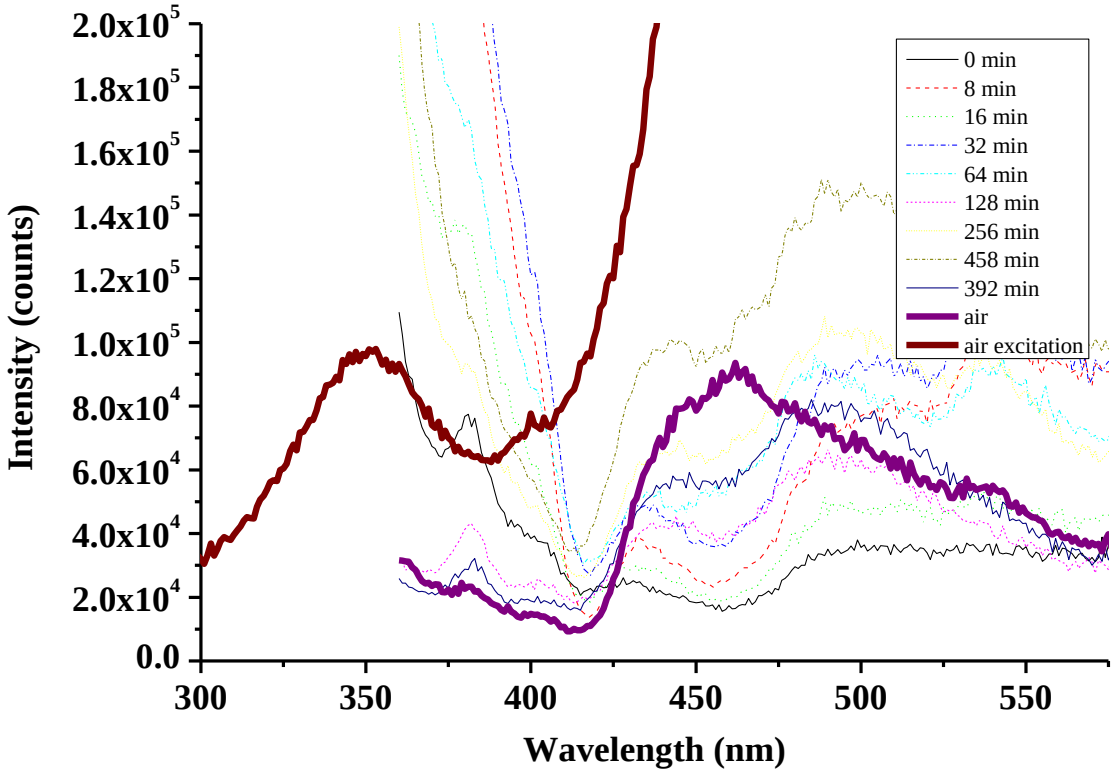

Figure 26 Photoluminescence emission (λ_{exc}=340 nm) and excitation spectra (($\lambda_{meas.}$= 460 nm) after different periods of irradiation time of a sample solution containing SnP (22 µM) and CoOxime (400 µM) in 0.2 M TEOA with 0.1 M sodium phosphate in water pH=7 irradiated at $\lambda_{irr} \geq 420$ nm; slit (5/5); The spectrum shown in bold lines was recorded after a photolysis time of 400 min and purging of the solution with air to oxidize Co(II) compounds in the solution in order to minimize their interference with the NADH emission. The sample shows weak emission with a maximum at 460 nm. The corresponding excitation spectrum shows a small intensity maximum at 360 nm which can be a hint for possible NADH formation according to related literature[46], but there is additional proof (UV-Vis absorbance or coupled enzymatic process) needed.

ZnP as sensitizer

Zinc (II) *meso*-tetrakis-(*N*-metylpyridinium) porphyrin was used as a sensitizer in the system inspired by the work of Lazarides et al.[45] who successfully applied **ZnP** but no formation of NADH could be observed in the system. Formation of hydrogen was significantly lower without addition of ACN to the solvent. The excited state reduction potential of **ZnP** is with -450 mV very close to what is necessary to reduce the cobaloxime complex with -430 mV for Co(III) to Co(II), so small changes in the pH or in the solvent might have big effects on the performance of the system.

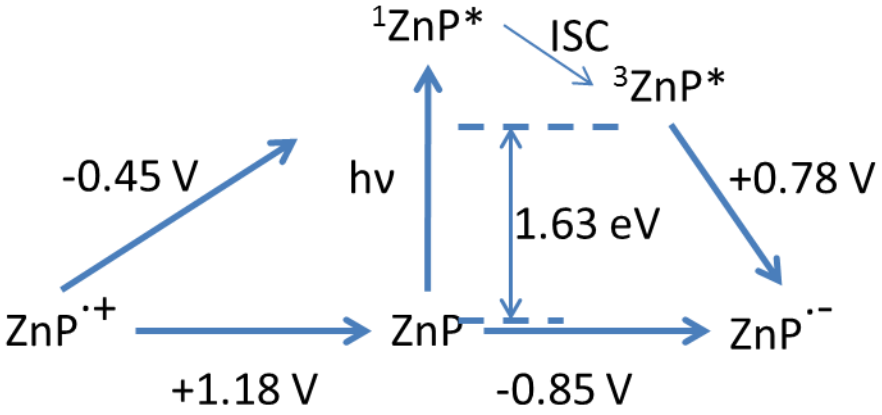

Figure 27 Energy diagram for the excited state redox potential of Zinc (II) *meso*-tetrakis-(*N*-metylpyridinium) porphyrin in aqueous solution[56]

ZnTSPP as sensitizer

The anionic Zinc (II) *meso*-tetrasulphonatophenyl porphyrin **ZnTSPP** was used instead of the cationic **ZnP** in order to observe if a more reducing porphyrin photosensitzers PS could possibly facilitate the electron transfer to the **CoOxime** and if some electrostatic interactions might influence the performance of the system in positive way, as eosin Y under the conditions applied here with pH 7 is also dianionic, with a pK_{a1} of 2.9 and pK_{a2} of 4.5.[61]

There were only trace amounts of hydrogen formed, no NADH could be detected.

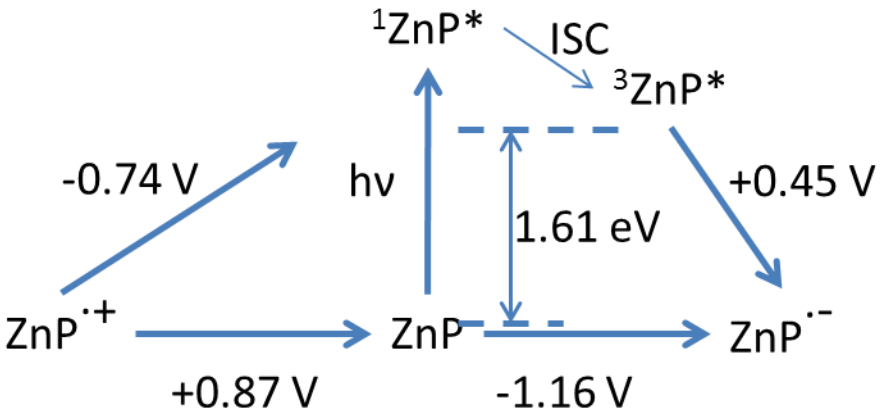

Figure 28 Energy diagram for the excited state redox potential of Zinc (II) *meso*-tetrasulphonatophenyl porphyrin in aqueous solution[56]

Ru(bpy)$_3^{2+}$ as sensitizer

Ruthenium-*tris*-bipyridine Ru(bpy)$_3^{2+}$ as a photosensitizer has quite similar optical properties and excited state redox potential to eosinY. So the compound was tested as photosensitizer in combination with cobaloxime under similar conditions as eosin Y with detection of hydrogen by GC as well as HPLC detection of NADH. No hydrogen was detected until an additional redox mediator methyl viologene (MV^{2+}) was added to the solution to facilitate the formation of hydrogen. The formation of NADH could not be observed under the conditions applied.

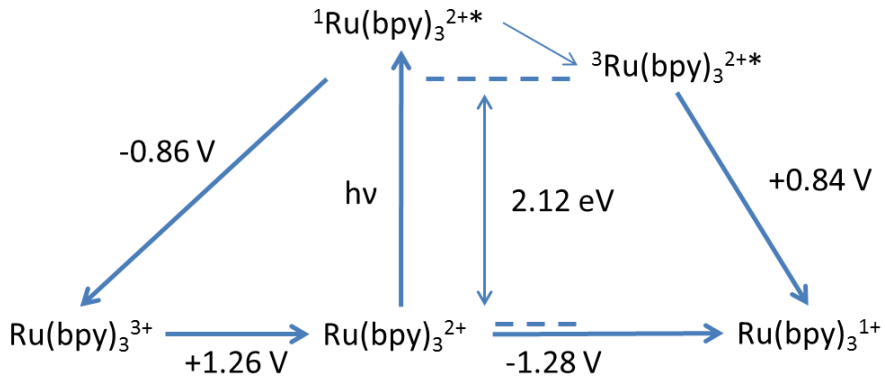

Figure 29 Energy diagram for the excited state redox potential of ruthenium-*tris*-bipyridine in water[62]

Summary on photolysis experiments for the formation of hydrogen and NADH

The photolysis experiments all showed various amounts of hydrogen formed in the solution, but besides the case of eosin Y as photosensitizer which showed some performance for both H^+ and NAD^+ reduction with ~100 % conversion after just 1 h upon use of a 10 fold excess of Eosin Y compared to cobaloxime. The turnover numbers (TN) and rates of hydrogen evolution (TOF) of the photosensitzers were below 100, except for eosin Y as a photosensitizer, in most cases below 10. The systems containing acetonitrile showed better performance in terms of hydrogen evolution as similar systems without acetonitrile, probably due to the stability of the cobaloxime compound.

Table 3 Summary on photolysis experiments (a more detailed summary can be found in the appendix)

PS	Catalyst	Solvent	H_2 (TN)	NADH	Remarks
Eosin Y	CoOx	ACN/water	yes (257)		0.2 M TEOA
Eosin Y	CoOx	water	yes	yes	0.2 M TEOA
Eosin Y		water	no	no	0.2 M TEOA
ZnTMPyP	CoOx	ACN/water	yes (75)	no	5% TEOA
ZnTMPyP	$Co(dmgBF_2)_2$	ACN/water	no	no	5% TEOA
SnTMPyP	CoOx	ACN/water	yes (5)	no	
SnTMPyP	CoOx	water	yes	no	
ZnTSPP	CoOx	water	yes (<1)	no	
ZnTSPP	CoOx	water	yes	no	
$Ru(bpy)_3^{2+}$	CoOx	water	no	no	
$Ru(bpy)_3^{2+}$	MV^{2+}/CoOx	water	yes	no	

No hydrogen or NADH was formed using $Co(dmgBF_2)_2$ as hydrogenation catalyst which can be explained by the redox potential connected to the rather high pH value (for this compound). For $Ru(bpy)_3^{2+}$ it was necessary to add an additional redox mediator methyl viologene (MV^{2+}) to the solution to facilitate the formation of hydrogen.

PL-Quenching Experiments

Photoluminescence quenching was performed and evaluated correction for increasing absorbance of the fluorescence quencher at the excitation wavelength of the emitting photosensitizer for the determination of the Stern-Volmer constant K_{SV} was were performed applying the equations below to determine with I as the emission intensity with increasing concentration $[Q]_i$ of quencher Q and A as optical absorption at the excitation wavelength.[63]

$$\frac{I_{em_0}}{I_{em_i}}\eta = 1 + K_{SV}\,[Q]_i$$

$$\eta = \frac{A_{x_0}\,(1 - 10^{-A_{x_i}})}{A_{x_i}\,(1 - 10^{-A_{x_0}})}$$

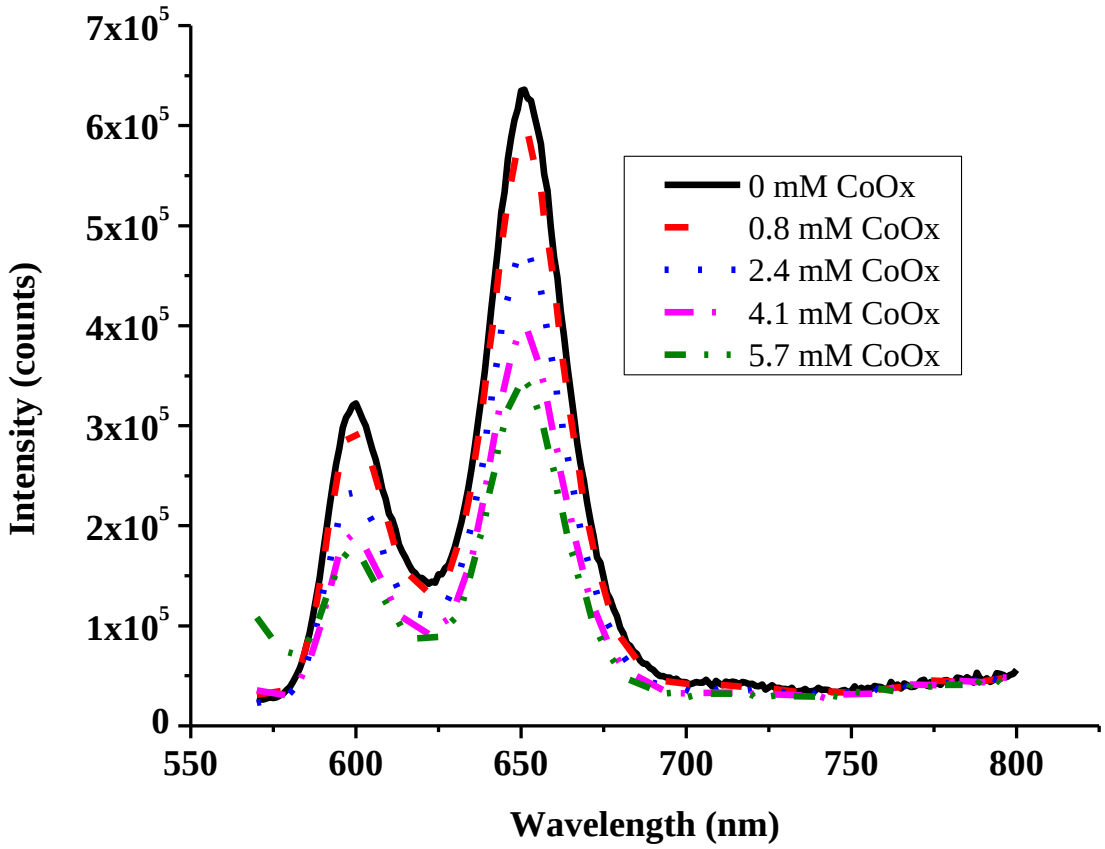

Figure 30 Photoluminescence quenching experiment with SnP and CoOxime in ACN/0.1 M phosphate buffer 1:1

The fluorescence quenching of the **SnP**-photosensitizer with a Stern-Volmer constant of Ksv = 169 ± 9 is not very efficient and the excited state triplet state of the porphyrin is known to be very well quenched reductively by TEOA. As the system containing **SnP** (and SnC) as photosensitzers were not that effective for the formation of hydrogen and did not show any performance for the formation of NADH there was no interest in performing triplet state quenching experiments with cobaloxime and **SnP** further on. Most likely the reductive quenching of the tin porphyrin by TEOA is much faster, than the oxidative quenching by **CoOxime** and additionally the quite high concentration of sacrificial donor TEOA compared to the concentration of the cobaloxime in the system hinders direct reduction of the cobaloxime by the excited state of the **SnP** quite significantly.

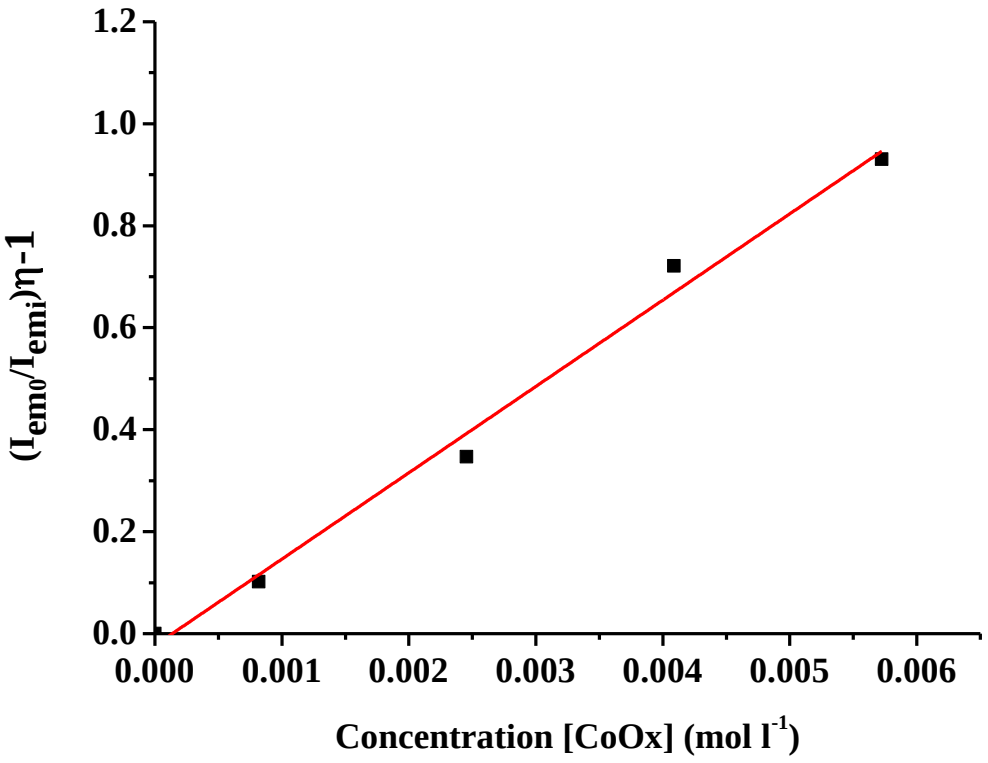

Figure 31 Stern-Volmer Plot for the fluorescence quenching experiment with SnP and CoOxime in ACN/0.1 M phosphate buffer 1:1, slope: K_{sv} = 169 ± 9.

Electrochemical Measurements

Electrochemical measurements were performed with the model compound *N*-benzyl-3-carbamoyl-pyridinium hexafluorophosphate **BNA** in anhydrous oxygen-free solutions with methanol as proton source in an otherwise non-protic solvent acetonitrile. The measurements should give some insight into the mechanism of the reduction of NAD^+ by cobaloxime in general.

Electrochemical Measurements- Cyclic Voltammetry

The cyclic voltammogram of cobaloxime (saturated solution) on glassy carbon (Figure 32) with **BNA** and methanol in 0.1 M $TBAPF_6$/ACN shows two additional quasi-reversible peaks at $E_{1/2}$ = -575 mV and $E_{1/2}$ = -1048 mV. The potential of the irreversible reduction of **BNA** at -813 mV does not change as methanol is added to the electrolyte solution and overlays with the reversible

reduction of the cobalt complex at $E_{1/2}$ = -875 mV. This redox couple, most Co(II)/Co(I)[36] shifts to more positive redox potential in absence of **BNA** upon addition of methanol to the electrolyte solution by about 30 mV, shows an weak additional wave at -750 mV and leads to catalytic reduction of methanol by Cobaloxime at -1.6 V.

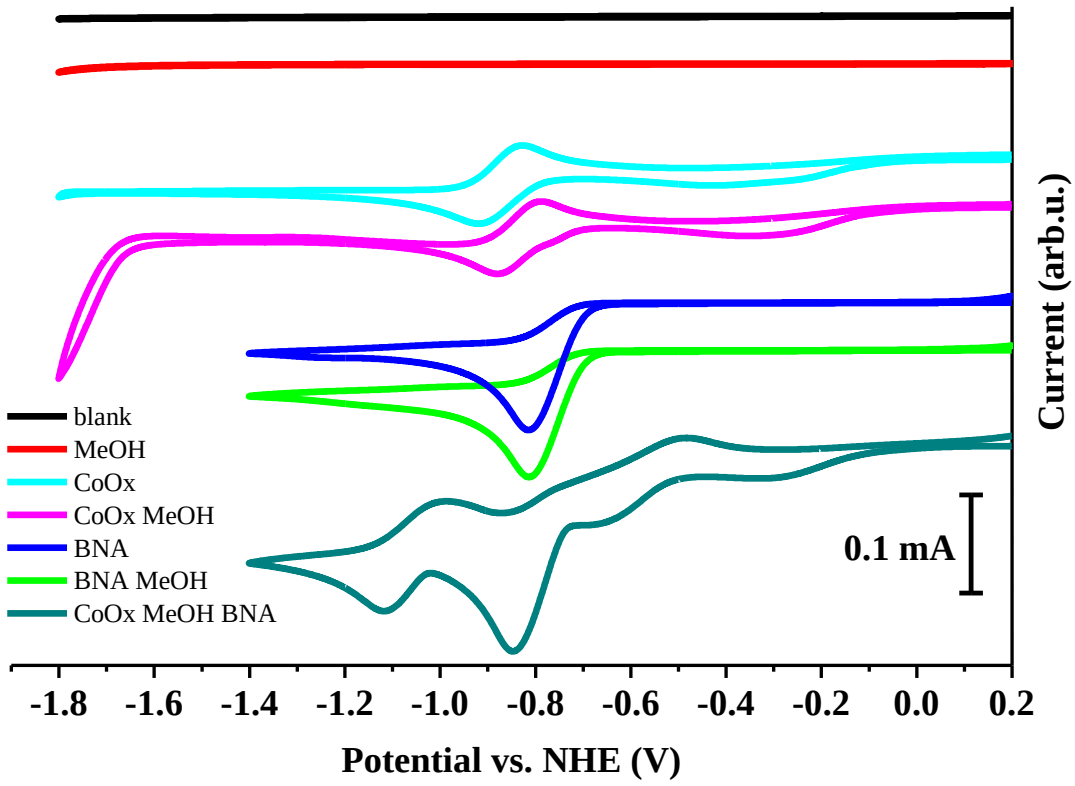

Figure 32 Cyclic voltammogram of a saturated CoOxime solution in 3 ml 0.1 M $TBAPF_6$ in dry acetonitrile with or without 0.1 ml methanol added. Addition of ~10 mg of BNA to the solution containing CoOxime, BNA and MeOH leads to the formation of two new reversible reductive waves.

Subsequent addition of small amount s of **BNA** into a saturated solution of **CoOxime** in 0.1 M $TBAPF_6$ in dry acetonitrile leads to a shift of the reversible reduction at $E_{1/2}$ = -875 mV of the Co(II) to Co(I)-species to more negative potential and to the formation of a second irreversible reduction at E_p = -1.12 V. The irreversible reduction of **BNA** to the $(\mathbf{BNA})_2$ dimer occurs around -800 mV vs. NHE.[9,64]

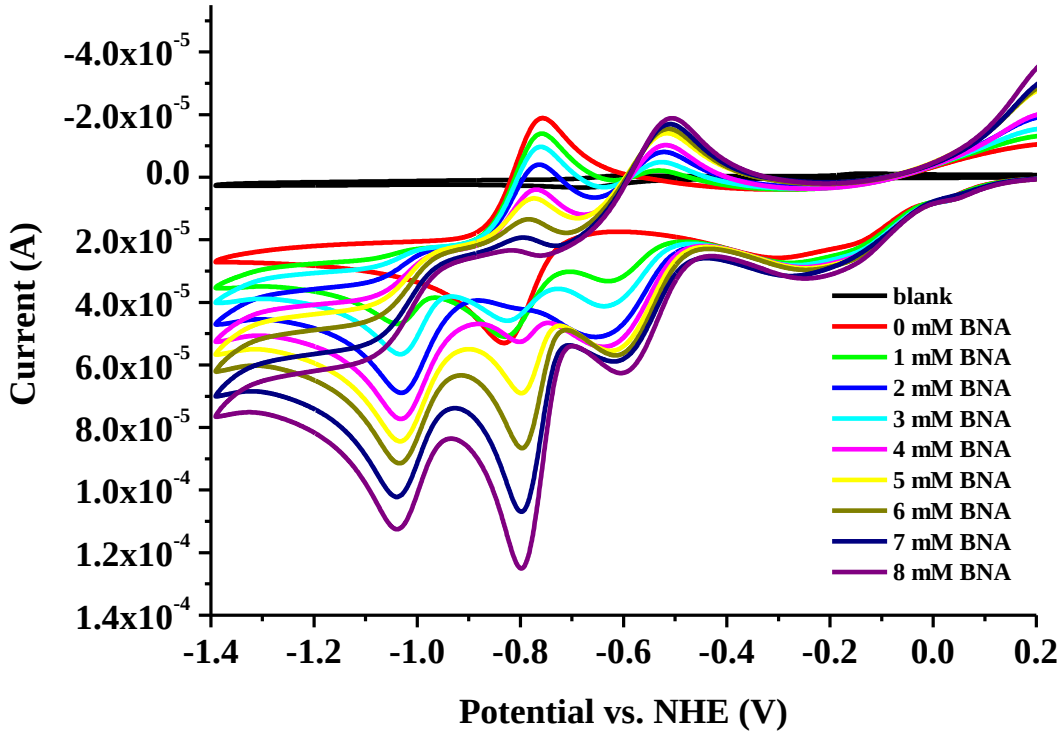

Figure 33 Cyclic voltammograms of CoOxime in 3 ml 0.1 M $TBAPF_6$ in dry acetonitrile with increasing amount of BNA added to the electrolyte solution

Electrochemical Measurements- Spectroelectrochemistry

UV-Vis spectroelectrochemical measurement done during controlled potential electrolysis CPE of **BNA** and cobaloxime at -650 mV vs. NHE in 0.1 M $TBAPF_6$ in acetonitrile calibrated with Fc/Fc^+ showed increasing absorbance at 360 nm which can indicate the electrocatalytic formation of **BNAH**, but the broad signal arising from 400 to 600 nm could not be assigned to that species and is most likely occurring due to reduced cobaloxime species in the solution. Further measurement of the electrolyzed solution with HPLC did not support formation of **BNAH**.

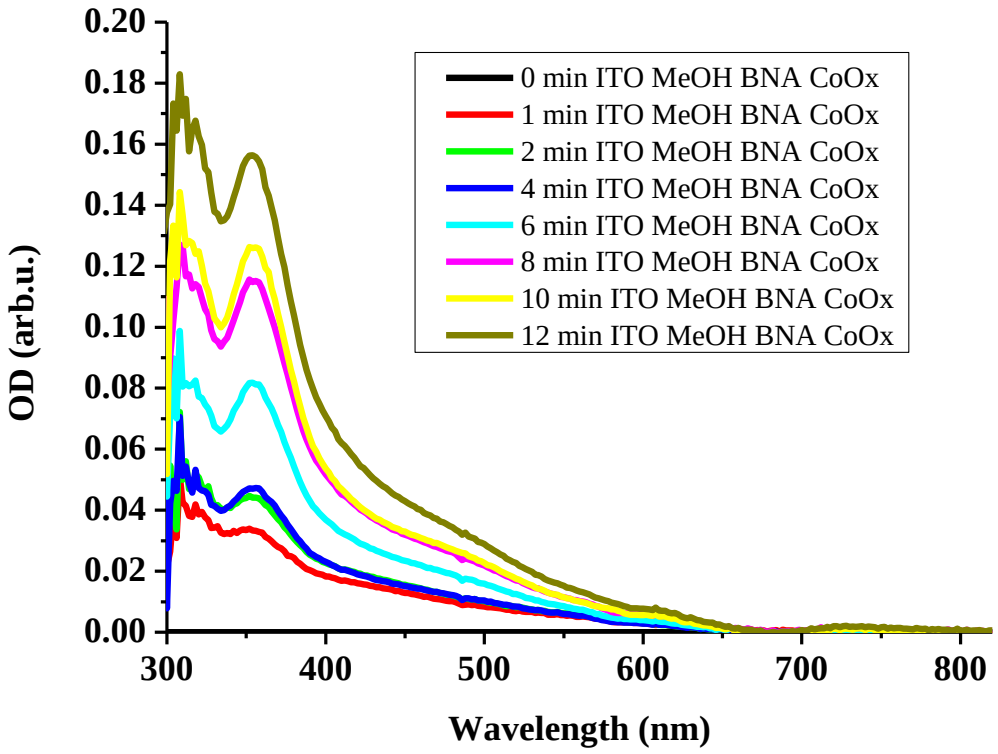

Figure 34 CPE at -650 mV vs. NHE in 0.1 M $TBAPF_6$ in acetonitrile calibrated with Fc/Fc^+; Increasing absorbance at 360 nm can indicate the electrocatalytic formation of BNAH, but the broad signal from 400 to 600 nm could not be assigned to that species and is most likely occurring due to reduced cobaloxime species in the solution.

Electrochemical Measurements- Bulk Electrolysis

A sample containing 0.3 ml methanol, 21.1 mg $BNAPF_6$ and 21.2 mg **CoOxime** in 6 ml 0.1 M $TBAPF_6$ was electrolyzed at a glassy carbon electrode for 1 h. Before and after the electrolysis cyclic voltammetry measurements were performed to determine reducible and oxidizable species in the solution. After the experiments also ferrocene was added for calibration of the reduction potential.

Redox potentials of reduced **BNA** species are[64–66]

- E^0_{ox}(4,4‘-BNA)$_2$ = 0.26 V vs. SCE (0.50 V vs. NHE) for the dimer and
- E^0_{ox}(**BNAH**)= 0.57 V vs. SCE (0.81 V vs. NHE) for the reduced cofactor model in acetonitrile solution.

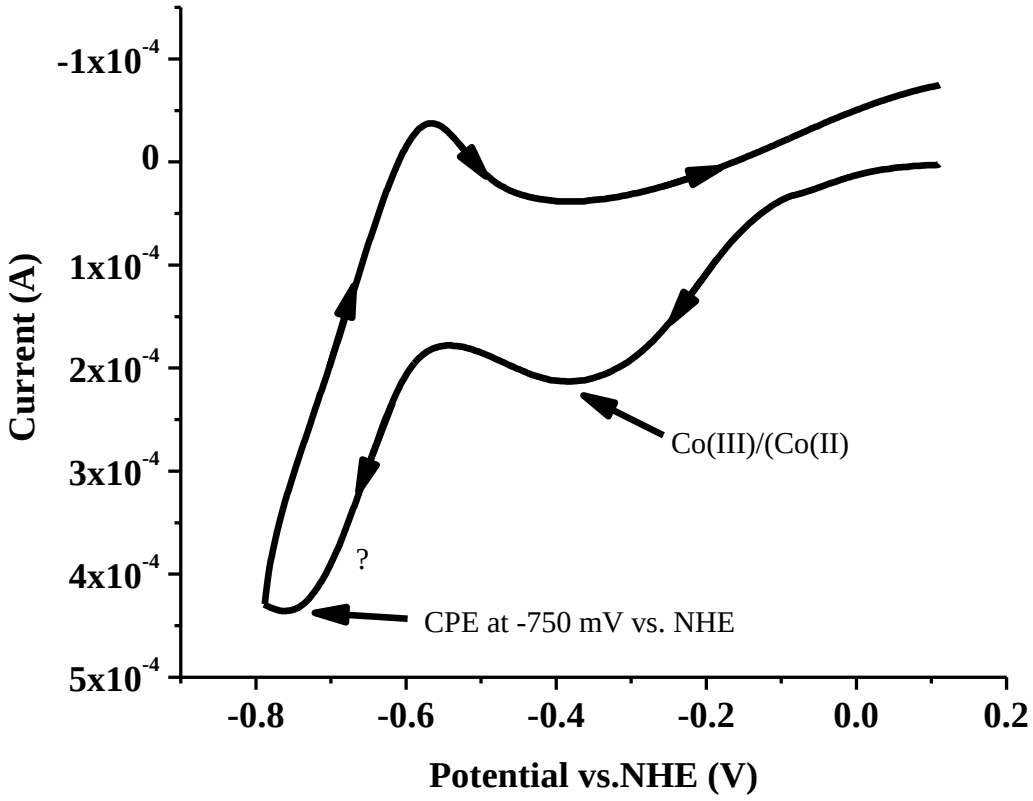

Figure 35 Cyclic voltammogram (50 mV s^{-1}) for the determination of the reduction potential for the controlled potential electrolysis for the formation BNAH.

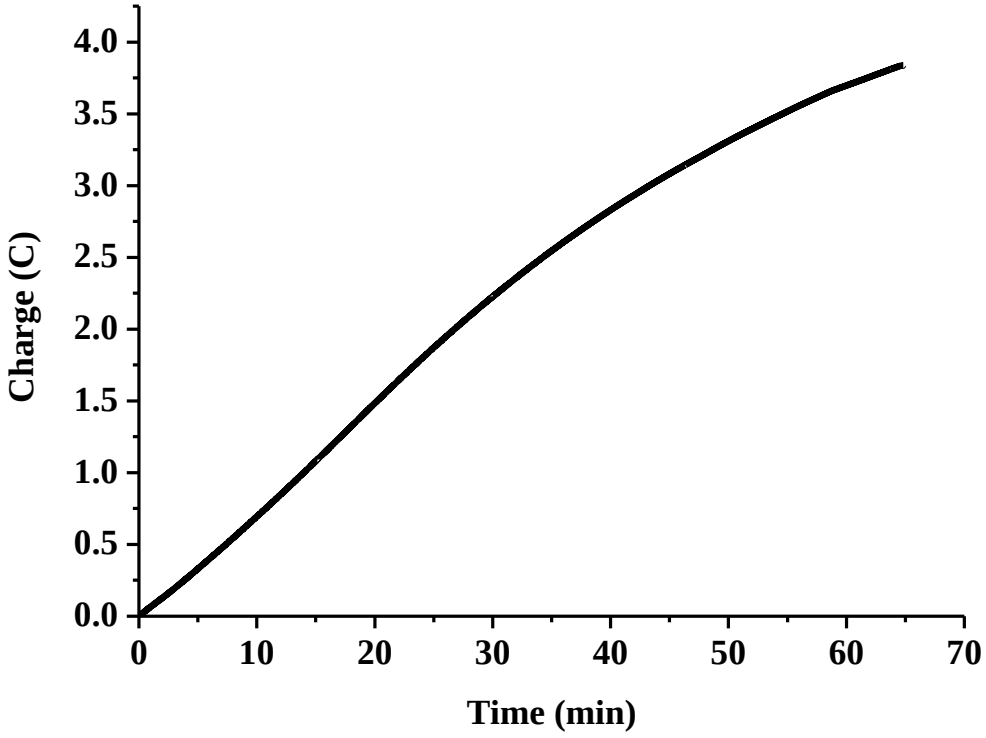

Figure 36 Time/charge curve for the controlled potential electrolysis of BNA and CoOxime in 0.1 M $TBAPF_6$ on a glassy carbon electrode at -750 mV vs. NHE; Total number of charges: 3.84 C after 63 min.

Reoxidation of the species formed in the bulk electrolysis in a cyclic voltammogram recorded right after stopping the electrochemical reduction process shown a single a single non reversible oxidation wave at 1023 mV vs. NHE together with a very weak signal at around 0.48 V. Both of these signals cannot be easily assigned to the formation of **BNAH** nor to oxidation of a dimer such as $(\mathbf{BNA})_2$ which are possibly formed via formation of a **BNA** radical followed by dimerization (see Figure 5 for more details). Upon comparison of the measured redox potentials with literature values for both species neither of them obviously fits to the measured oxidation potential. So there must be some other species be formed by the reaction.

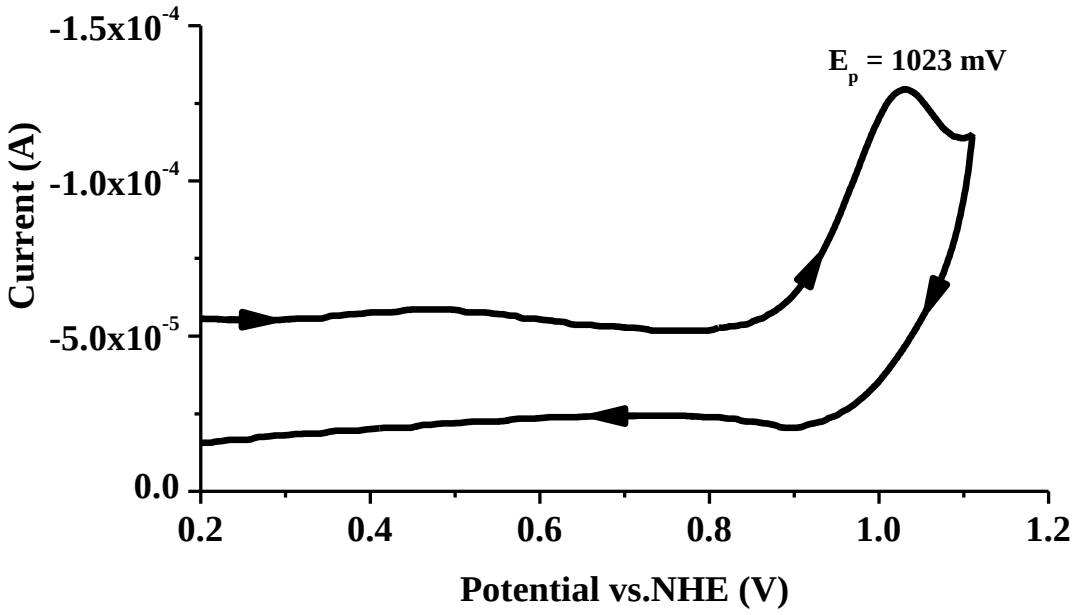

Figure 37 Oxidative cyclic voltammogram recorded after 10 min of controlled potential electrolysis of a solution containing BNA, CoOxime and MeOH as proton source shows a single non reversible oxidation wave at 1023 mV vs. NHE.

Additional HPLC detection concerning **BNAH** could also detect neither BNAH nor the dimer conclusively.

Conclusions

Photolysis experiments performed here and reported in the literature[43,45] have shown that there is some potential for both cationic **SnP** and **ZnP** porphyrins to perform as sensitizer for the reduction of water with a cobaloxime complex. What can be seen from the performed experiments so far, that a large excess of cobaloxime (S:C = 1:20) is beneficial for an effective water reduction system, as well as reasonably high donor concentrations, this can be optimized, but the overall yields, especially of enzymatically active NADH might be limited. This is especially due to the fact that a high amount of reduced cobaloxime intermediates in the solution would favour homolytic bond breaking and following a dimeric pathway for the formation of hydrogen rather than the formation of a necessary hydride. The fixation of the cobaloxime on a (photosensitizing) substrate might be useful to hinder bimolecular pathways and make a necessary hydride or 2 e^--PCET (proto coupled electron transfer) more likely.[67]

It is possible that at least some very small amount of NADH is formed in the photolysis process where **SnP** is applied, but the detection methods have to be expanded. As the absorbance of cobalt catalyst intermediates interferes with photoluminescence detection of NADH chromatographic detection methods have proven to be useful to exclude other reduced cofactor species with similar absorption properties. Those species can easily be mistaken for NADH.

It is known from the literature that for tin(IV) porphyrins **SnP** in most cases the lowest lying triplet state is the most likely excited state to be quenched and to participate in photochemical reactions as these molecules have a high intersystem crossing rate (0.95) and a relatively long triplet state lifetime: T_1-T_N absorption shows a maximum at 460 nm and the lifetime of the T_1 state has been measured to be 0.92 ms.[68] The tin porphyrin is very easily reduced[69] and thus prone to be reductively quenched by TEOA as a sacrificial donor which can be a reason for the weak performance of the porphyrin in combination with the cobaloxime.

Electrochemical Measurements have shown that the reversible Co(II)/Co(I) couple cannot be easily used for the reduction of **BNA** but that the addition of **BNA** to a solution of reduced cobaloxime leads to some coupled (electro)chemical reactions, the interpretation of the performed measurements needs deeper investigation. Even measurements of the reduction

product via spectroelectrochemistry and bulk electrolysis coupled with HPLC did not yield totally conclusive answers about the nature of the product of the electrochemical reduction.

An experiment with **SnP**/**CoOxime** without NAD^+ in purely aqueous solvent was tried, as the photolysis of a solution containing all three components showed reasonably high amounts of hydrogen compared to what was observed a purely aqueous system by Kim et al.[46] who reported merely 15 turnovers after 5 h of irradiation of their system with Eosin Y, but did with only 8 turnovers after 500 min also not yield such high amounts of hydrogen.

Enhancement of the ratio **SnP**/**CoOxime** and aeration of photolysis solution in shorter time intervals in order to oxidize the interfering Co(II) species absorbing close to the emission wavelength of NADH prior to fluorescence measurement can improve the detection of NADH via UV-Vis or luminescence measurements but HPLC seems to be the only reliable method for direct cofactor detection from the solution when it comes to higher concentrations of **CoOxime**, photosensitizer and NADH.

Photolysis experiments including formation of phlorin prior addition of **CoOxime** could be good, as well as to try other sacrificial donors, for example some that form radical anions upon reductive quenching of the **SnP*** states.

The stability of the **CoOxime** as hydrogenation catalyst in purely aqueous solvent is very limited, so the stability of the cobalt catalyst has to be improved to be applicable under physiological conditions if the system should be coupled to enzymatic processes in larger scale. There are other cobalt catalysts such as porphyrins that might fulfil this property better.

Acknowledgements

I want to thank the Austrian Marshall Plan Foundation for funding my interesting stay at the Brookhaven National Laboratory in Long Island, NY and the whole Artificial Photosynthesis group led by Dr. Etsuko Fujita for their hospitality.

I want to specially thank Dr. Etsuko Fujita and Dr. James Muckerman for their hospitality at Thanksgiving and otherwise! Big thanks go to Dr. Yasuo Matsubara for lending his precious equipment to me as well as fruitful discussions about the project and instructions for the use of lab equipment.

I want to specially mention Dr. Dmitry Polyansky, Dr. Javier Concepcion and Dr. Anna Lewandowska as well as BSc. Barbara Mello for supporting me with my project.

Thanks to Dr. Wei-Fu Chen and Dr. Chloe Chen for taking me out to ski and to show me some not so well known parts of NYC! Thanks to all other members of the AP group at BNL!

I also want to thank my supervisor Prof. Dr. Günther Knör, for the possibility to leave the lab at the JKU for some time to perform this research project at such a special place!

References

(1) Ferreira, K. N.; Iverson, T. M.; Maghlaoui, K.; Barber, J.; Iwata, S. *Science (80-.).* **2004**, *303*, 1831.

(2) Umena, Y.; Kawakami, K.; Shen, J.-R.; Kamiya, N. *Nature* **2011**, *473*, 55.

(3) Knör, G. *Chem. – A Eur. J.* **2009**, *15*, 568.

(4) Knör, G.; Monkowius, U. *Adv. Inorg. Chem.* **2011**, *63*, 235.

(5) Nelson, D.; Cox, M. *Lehninger Biochemie*; 3rd ed.; Springer: Berlin Heidelberg, 2001; pp. 519–565.

(6) Chenault, H. K.; Whitesides, G. *Appl. Biochem. Biotechnol.* **1987**, *14*, 147.

(7) Lo, H. C.; Buriez, O.; Kerr, J. B.; Fish, R. H. *Angew. Chem. Int. Ed.* **1999**, *38*, 1429.

(8) Lo, H. C.; Leiva, C.; Buriez, O.; Kerr, J. B.; Olmstead, M. M.; Fish, R. H. *Inorg. Chem.* **2001**, *40*, 6705.

(9) Lo, H. C.; Fish, R. H. *Angew. Chem. Int. Ed.* **2002**, *41*, 478.

(10) Kölle, U.; Grätzel, M. *Angew. Chem. Int. Ed.* **1987**, *26*, 567.

(11) Kölle, U.; Kang, B.-S.; Infelta, P.; Comte, P.; Grätzel, M. *Chem. Ber.* **1989**, *122*, 1869.

(12) Hollmann, F.; Witholt, B.; Schmid, A. *J. Mol. Catal. B Enzym.* **2003**, *19-20*, 167.

(13) Hollmann, F.; Hofstetter, K.; Schmid, A. *Trends Biotechnol.* **2006**, *24*, 163.

(14) Lutz, J.; Hollmann, F.; Ho, T. V.; Schnyder, A.; Fish, R. H.; Schmid, A. *J. Organomet. Chem.* **2004**, *689*, 4783.

(15) Hollmann, F.; Arends, I. W. C. E.; Buehler, K. *ChemCatChem* **2010**, *2*, 762.

(16) Grau, M. M.; Poizat, M.; Arends, I. W. C. E.; Hollmann, F. *Appl. Organomet. Chem.* **2010**, *24*, 380.

(17) Poizat, M.; Arends, I. W. C. E.; Hollmann, F. *J. Mol. Catal. B Enzym.* **2010**, *63*, 149.

(18) Shi, Q.; Yang, D.; Jiang, Z.; Li, J. *J. Mol. Catal. B Enzym.* **2006**, *43*, 44.

(19) Lee, S. H.; Ryu, J.; Nam, D. H.; Park, C. B. *Chem. Commun.* **2011**, *47*, 4643.

(20) Lee, S. H.; Nam, D. H.; Park, C. B. *Adv. Synth. Catal.* **2009**, *351*, 2589.

(21) Lee, S. H.; Nam, D. H.; Kim, J. H.; Baeg, J.-O.; Park, C. B. *ChemBioChem A Eur. J. Chem. Biol.* **2009**, *10*, 1621.

(22) Kim, J. H.; Lee, S. H.; Lee, J. S.; Lee, M.; Park, C. B. *Chem. Commun.* **2011**, *47*, 10227.

(23) Nam, D. H.; Park, C. B. *ChemBioChem* **2012**, *13*, 1278.

(24) Kozuch, S.; Martin, J. M. L. *ACS Catal.* **2012**, *2*, 2787.

(25) Buchler, J. W. In *The Porphyrins, Vol. 1*; Dolphin, D., Ed.; Academic Press: New York, 1978; p. 390.

(26) Knör, G. *Coord. Chem. Rev.* **1998**, *171*, 61.

(27) Arnold, D. P.; Blok, J. *Coord. Chem. Rev.* **2004**, *248*, 299.

(28) Krüger, W.; Fuhrhop, J.-H. *Angew. Chem.* **1982**, *94*, 132.

(29) Handman, J.; Harriman, A.; Porter, G. *Nature* **1984**, *307*, 534.

(30) Whitten, D. G.; Yau, J. C. N.; Carroll, F. *J. Am. Chem. Soc.* **1971**, *93*, 2291.

(31) Harriman, A. *J. Photochem.* **1985**, *29*, 139.

(32) Kalyanasundaram, K. *Inorg. Chem.* **1984**, *23*, 2453.

(33) Oppelt, K. T.; Wöß, E.; Stiftinger, M.; Schöfberger, W.; Buchberger, W.; Knör, G. *Inorg. Chem.* **2013**, *52*, 11910.

(34) Grätzel, M.; Moser, J.-E. In *Electron Transfer in Chemistry*; Wiley-VCH Verlag GmbH, 2001; pp. 588–644.

(35) Dixon, J. M.; Taniguchi, M.; Lindsey, J. S. *Photochem. Photobiol.* **2007**, *81*, 212.

(36) Dempsey, J. L.; Brunschwig, B. S.; Winkler, J. R.; Gray, H. B. *Acc. Chem. Res.* **2009**, *42*, 1995.

(37) Muckerman, J. T.; Fujita, E. *Chem. Commun. (Camb).* **2011**, *47*, 12456.

(38) Lazarides, T.; McCormick, T.; Du, P.; Luo, G.; Lindley, B.; Eisenberg, R. *J. Am. Chem. Soc.* **2009**, *131*, 9192.

(39) McCormick, T. M.; Calitree, B. D.; Orchard, A.; Kraut, N. D.; Bright, F. V; Detty, M. R.; Eisenberg, R. *J. Am. Chem. Soc.* **2010**, *132*, 15480.

(40) Gong, L.; Wang, J.; Li, H.; Wang, L.; Zhao, J.; Zhu, Z. *Catal. Commun.* **2011**, *12*, 1099.

(41) Natali, M.; Orlandi, M.; Chiorboli, C.; Iengo, E.; Bertolasi, V.; Scandola, F. *Photochem. Photobiol. Sci.* **2013**, *12*, 1749.

(42) Zhang, P.; Wang, M.; Li, X.; Cui, H.; Dong, J.; Sun, L. *Sci. China Chem.* **2012**, *55*, 1274.

(43) Zhang, P.; Wang, M.; Li, C.; Li, X.; Dong, J.; Sun, L. *Chem. Commun.* **2010**, *46*, 8806.

(44) Du, P.; Knowles, K.; Eisenberg, R. *J. Am. Chem. Soc.* **2008**, *130*, 12576.

(45) Lazarides, T.; Delor, M.; Sazanovich, I. V.; McCormick, T. M.; Georgakaki, I.; Charalambidis, G.; Weinstein, J. A.; Coutsolelos, A. G. *Chem. Commun.* **2014**, *50*, 521.

(46) Kim, J. A.; Kim, S.; Lee, J.; Baeg, J.-O. *Inorg. Chem.* **2012**, *51*, 8057.

(47) Steckhan, E.; Herrmann, S.; Ruppert, R.; Dietz, E.; Frede, M.; Spika, E. *Organometallics* **1991**, *10*, 1568.

(48) Steckhan, E. In *Electrochemistry V SE - 3*; Steckhan, E., Ed.; Topics in Current Chemistry; Springer Berlin Heidelberg, 1994; Vol. 170, pp. 83–111.

(49) Dempsey, J. L.; Winkler, J. R.; Gray, H. B. *J. Am. Chem. Soc.* **2010**, *132*, 1060.

(50) Dempsey, J. L.; Winkler, J. R.; Gray, H. B. *J. Am. Chem. Soc.* **2010**, *132*, 16774.

(51) McCormick, T. M.; Han, Z.; Weinberg, D. J.; Brennessel, W. W.; Holland, P. L.; Eisenberg, R. *Inorg. Chem.* **2011**, *50*, 10660.

(52) Eckenhoff, W. W. T.; McNamara, W. R. W.; Du, P.; Eisenberg, R. *Biochim. Biophys. Acta - Bioenerg.* **2013**, *1827*, 958.

(53) Harriman, A.; Porter, G.; Walters, P. *J. Chem. Soc. Faraday Trans. 1 Phys. Chem. Condens. Phases* **1983**, *79*, 1335.

(54) Amao, Y.; Watanabe, T. *Appl. Catal. B Environ.* **2009**, *86*, 109.

(55) Hans Bisswanger. *Practical Enzymology*; 2nd ed.; WILEY-VCH Verlag & Co. KGaA: Weinheim, 2011.

(56) Kalyanasundaram, K.; Neumann-Spallart, M. *J. Phys. Chem.* **1982**, *86*, 5163.

(57) Gouterman, M. *J. Mol. Spectrosc.* **1961**, *6*, 138.

(58) Connelly, N. G.; Geiger, W. E. *Chem. Rev.* **1996**, *96*, 877.

(59) Gamry Instruments. Reference Electrodes http://www.gamry.com/products/accessories/reference-electrodes/.

(60) Neumann, M.; Füldner, S.; König, B.; Zeitler, K. *Angew. Chem. Int. Ed.* **2011**, *50*, 951.

(61) R.W. Sabnis. *Handbook of Acid-Base Indicators*; 10th ed.; CRC Press: Boca Raton, 2009; pp. 139–140.

(62) Kalyanasundaram, K. *Coord. Chem. Rev.* **1982**, *46*, 159.

(63) Borissevitch, I. E. *J. Lumin.* **1999**, *81*, 219.

(64) Patz, M.; Kuwahara, Y.; Suenobu, T.; Fukuzumi, S. *Chem. Lett.* **1997**, *26*, 567.

(65) Fukuzumi, S.; Ohkubo, K.; Fujitsuka, M.; Ito, O.; Teichmann, M. C.; Maisonhaute, E.; Amatore, C. *Inorg. Chem.* **2001**, *40*, 1213.

(66) Fukuzumi, S.; Koumitsu, S.; Hironaka, K.; Tanaka, T. *J. Am. Chem. Soc.* **1987**, *109*, 305.

(67) Lakadamyali, F.; Kato, M.; Muresan, N. M.; Reisner, E. *Angew. Chem. Int. Ed.* **2012**, *51*, 9381.

(68) Harriman, A.; Walters, P. *Inorg. Chim. Acta* **1984**, *83*, 151.

(69) Harriman, A.; Richoux, M. C.; Neta, P. *J. Phys. Chem.* **1983**, *87*, 4957.

Appendix

Table 4 Summary of photolysis experiments in which headspace samples were measured with GC

No.	Sensitizer	Cobaloxime	S:C	Solvent/ Donor	λ_{irr}	TN nH_2/ nS	Irr. Time/ Remarks
1	Eosin Y (15 µM)	CoOxime	1:27	ACN/0.2 M TEOA with 0.1 M sodium phosphate in water pH = 7	≥ 420 nm	257	128 min
2	Eosin Y (15 µM)	CoOxime (32 µM)	1:2	0.2 M TEOA with 0.1 M sodium phosphate in water pH = 7	≥ 420 nm	-	20 min, bleached
3	SnP (22 µM)	CoOxime (330 µM)	1:15	ACN/0.2 M TEOA with 0.1 M sodium phosphate in water pH = 7	≥ 540 nm	-	128 min bleached
4	SnP (22 µM)	CoOxime (330 µM)	1:15	ACN/0.2 M TEOA with 0.1 M sodium phosphate in water pH = 7	≥ 380 nm	2	160 min
5	SnP (22 µM)	CoOxime (400 µM)	1:18	ACN/0.2 M TEOA with 0.1 M sodium phosphate in water pH = 7	≥ 420 nm	5.5	400 min
6[a]	SnP (22 µM)	CoOxime (400 µM)	1:18	ACN/0.2 M TEOA with 0.1 M sodium phosphate in water pH = 7	≥ 420 nm	4	220 min
7[a]	SnP (22 µM)			ACN/0.2 M TEOA with 0.1 M sodium phosphate in water pH = 7	≥ 420 nm	-	32 min bleached
7[b,c]	SnC (22 µM)			0.2 M TEOA with 0.1 M sodium phosphate in water pH = 7	≥ 600 nm	-	12 h

No.	Sensitizer	Cobaloxime	S:C	Solvent/ Donor	λ_{irr}	TN nH_2/ nS	Irr. Time/ Remarks
8[c,d]	SnC (22 µM)	CoOxime (400 µM)	1:18	0.2 M TEOA with 0.1 M sodium phosphate in water pH = 7	≥ 600 nm	-	80 min
8[c,d]	SnP (22 µM)	CoOxime (360 µM)	1:16	0.2 M TEOA with 0.1 M sodium phosphate in water pH = 7	≥ 400 nm	8	500 min
9	ZnP (40 µM)	CoOxime (170 µM)	1:4	ACN/ 10% TEOA water pH = 7	≥ 440 nm	20	16 h
10	ZnP (40 µM)	CoOxime (420 µM)	1:10	ACN/ 10% TEOA water pH = 7	≥ 440 nm	75	28 h
11[e]	ZnP (40 µM)	CoOxime (420 µM)	1:10	ACN/ 10% TEOA water pH = 7	≥ 440 nm	25	4 h
12	ZnP (40 µM)	$Co(dmgBF_2)_2$ (420 µM)	1:10	ACN/10% TEOA water pH = 7	≥ 440 nm	-	25 h
13[f]	ZnP (40 µM)	CoOxime (420 µM)	1:10	ACN/10% TEOA water pH = 7	≥ 440 nm	-	18 h
14	ZnP (40 µM)	CoOxime (420 µM)	1:10	water/10% TEOA water pH = 7	≥ 440 nm	-	127 min

[a] solution also contained 0.6 mM NAD^+; [b] preparation on **SnC** via photolysis ($\lambda_{irr} \geq 420$ nm) of SnP under constant purging with ambient air previous to the photolysis; [b] solution also contained 1.2 mM NAD^+; [d] preparation on **SnC** via photolysis ($\lambda_{irr} \geq 450$ nm) of **SnP** under constant purging with ambient air previous to the photolysis; [e] photolysis was performed in a gas tight cell; [f] sample contained additional dimethylglyoxime: **CoOxime**:dmg = 1:5;